Assessing the waste heat recovery potential of liquid organic hydrogen carrier chains

Li, Longquan; Vellayani Aravind, Purushothaman; Woudstra, Theo; van den Broek, Machteld

Published in:
Energy Conversion and Management

DOI:
10.1016/j.enconman.2022.116555

Publication date:
2023

Energy Conversion and Management 276 (2023) 116555

Contents lists available at ScienceDirect

Energy Conversion and Management

journal homepage: www.elsevier.com/locate/enconman

Assessing the waste heat recovery potential of liquid organic hydrogen carrier chains

Longquan Li *, Purushothaman Vellayani Aravind, Theo Woudstra, Machteld van den Broek

Energy and Sustainability Research Institute Groningen, University of Groningen, 9747 AG Groningen, Netherlands

ARTICLE INFO

Keywords:
Liquid organic hydrogen carrier
Thermodynamic modeling
Waste heat recovery
Exergy analysis
Thermal energy management
Hydrogen storage

ABSTRACT

Proper thermal management can improve the efficiency of hydrogen storage chains based on liquid organic hydrogen carriers (LOHC). The energy and exergy efficiencies of 24 LOHC chains, which are differentiated by two hydrogen sources (S_{EL}: hydrogen from electrolyzer and $S_{INDU:}$ industrial by-product), three hydrogen consumers (C_{PEMFC}: proton exchange membrane fuel cell, C_{SOFC}: solid oxide fuel cell, and C_{INDU}: industrial consumer), and four LOHC pairs are calculated based on thermodynamic modeling. Possible strategies for the heat integration between the heat sources (including hydrogenation heat, heat generated by hydrogen consumer, and the high-temperature LOHC fluids) and the heat sinks (including LOHC preheating, hydrogen preheating, dehydrogenation, and external heating purposes) are designed for these chains. In the four selected LOHC pairs, dibenzyltoluene (DBT) is found to be the most favorable LOHC pair for the implementation of WHR strategies, mainly because of low heat demand for preheating (8.9% of the stored hydrogen energy) and a high dehydrogenation rate. The WHR strategies significantly improve the energy efficiency of LOHC chains by up to 21.7% points for the chains with C_{INDU} and 40.8% points for chains with C_{SOFC} or C_{PEMFC}, which makes LOHC chains more efficient than traditional compressed or liquid hydrogen chains in several scenarios, i.e., the DBT chain with C_{PEMFC} have the highest energy efficiency (70.4% for S_{EL}/69.5% for S_{INDU}), while the DBT chain with S_{INDU} and C_{SOFC} has the highest exergy efficiency (60.6%). For the remaining combinations of the remaining hydrogen sources and consumers, the compressed hydrogen chains are the most efficient.

1. Introduction

To reduce the risks and impacts of climate change, with the Paris Agreement adopted by 196 Parties, the increase in the global average temperature should be held well below 2 °C above pre-industrial levels, and efforts to limit the temperature increase to 1.5 °C should be pursued [1]. Parties are encouraged to strengthen their emissions reductions and to align their national climate action pledges with the most recent Glasgow Climate Pact [2]. Increasing the penetration of renewable energy sources is essential for a sustainable energy system [3]. The total capacity of renewable energies globally has risen from 1,224 GW in 2010 to 2,802 GW in 2020, with the entire renewable energy production of 4,202 TWh in 2010 and 6,963 TWh in 2019 [4,5]. In the Planned Energy Scenario proposed by the International Renewable Energy Agency, the share of modern renewable energies in the final energy supply would increase to 17 % by 2030 and 25 % by 2050. In the Transforming Energy Scenario, this share would increase to 28 % by 2030 and 66 % by 2050 [6]. Some renewable energy sources like wind and solar depend strongly on site-specific meteorological conditions and vary regionally and globally, making energy storage and transportation systems necessary [7].

Hydrogen is a promising energy carrier that can be produced from renewable energy sources, fossil fuels, or nuclear energy [8–20]. Fuel cells or combustion engines can use hydrogen to generate power without emissions [21]. Hydrogen can also support the decarbonization of hard-to-abate sectors, including the chemical, petroleum refining, and steel sectors [21–24]. Hydrogen and hydrogen-based fuels accounted for < 0.1 % of total energy consumption in 2020 and are predicted to increase to 2 % in 2030 and 10 % in 2050 [25]. Hydrogen can be stored in the forms of compressed hydrogen gas (CHG), liquid/cryogenic hydrogen (LH), cryo-compressed hydrogen, metal hydride, carbon nanotubes, metal–organic frameworks, and liquid organic hydrogen carriers (LOHC) [8,26], with each having their advantages and shortcomings [7,26–28]. Storing hydrogen within LOHC is based on reversible chemical reactions of hydrogenation and subsequent dehydrogenation

* Corresponding author at: Energy Academy Europe building, Nijenborgh 6, 9747 AG Groningen, Netherlands.
E-mail addresses: longquan.li@rug.nl (L. Li), a.purushothaman.vellayani@rug.nl (P. Vellayani Aravind), t.h.woudstra@rug.nl (T. Woudstra), m.a.van.den.broek@rug.nl (M. van den Broek).

https://doi.org/10.1016/j.enconman.2022.116555
Received 23 September 2022; Received in revised form 12 November 2022; Accepted 4 December 2022
Available online 14 December 2022

Nomenclature

C_p	Heat capacity (J/(kg • K))
e	Exergy per mass flow rate (J/kg)
h	Enthalpy (J/kg)
H	Hydrogen
k	Specific heat ratio of hydrogen
$\dot{m}$	Mass flow rate (kg/s)
M	Molar mass (kg/mol)
N	Number of compressor stages
p	Pressure (MPa)
P	Electricity consumption (MW)
q	Reaction heat per mole hydrogen (kJ/mol H_2)
Q	Heat (MW)
R	Universal gas constant
s	Entropy (J/K)
T	Temperature (K)
Z	Compressibility factor
ΔT	Temperature rise (K)

Subscripts

0	Ambient
1	Number of preheaters
2	Number of preheaters
3	Number of preheaters
4	Number of preheaters
c	Coolant
ch	Chemical
Comp	Compressor
de	Dehydrogenation
EL	Electrolyzer
FC	Fuel cell
h	Heat
H	Hydrogen preheater
hy	Hydrogenation
H_2	Hydrogen
in	Input
is	Isentropic
INDU	Industrial
L+	Loaded LOHC
L-	Unloaded LOHC
m	Mass flow
me	Mechanical
mini	Minimum
out	Exiting
ph	Physical
q	Heat flow
r	Reusable
SMR	Steam methane reforming
suc	Suction

Superscripts

C	Hydrogen consumers
Ex	Exergy
En	Energy
e	Exergy per mass flow rate
S	Hydrogen sources
H	Hydrogen

Greek letters

η	Efficiency
∂	Stoichiometric ratio of H_2 to LOHC

Abbreviations

CHG	Compressed hydrogen gas
HHV	Higher heating value
LH	Liquified hydrogen
LHV	Lower heating value
LOHC	Liquid organic hydrogen carrier
PEMFC	Proton exchange membrane fuel cell
SOFC	Solid oxide fuel cell
WHR	Waste heat recovery

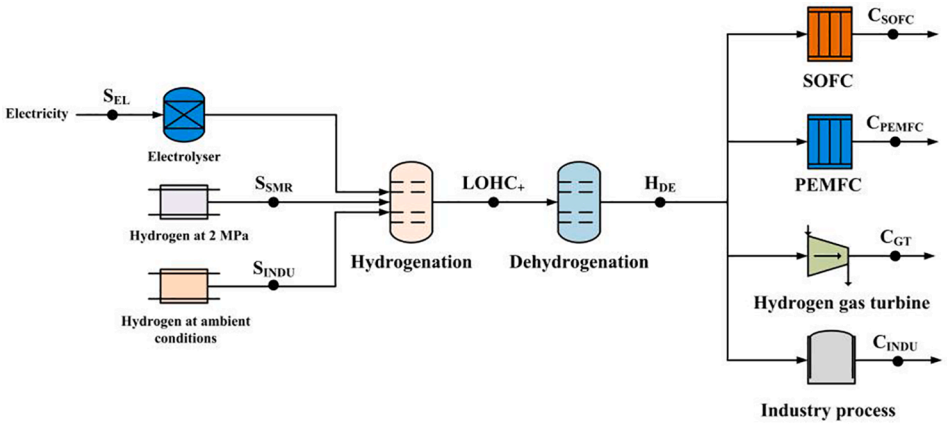

Fig. 1. Potential chains enabled by LOHC.

of organic molecules. The excess hydrogen reacts with the unloaded LOHC in a hydrogenation reactor, and a dehydrogenation reactor releases the stored hydrogen in the loaded LOHC when needed. Fig. 1 shows potential chains based on LOHC in the literature. Hydrogen produced by electrolyzers, steam methane reforming, or as an industrial product can be consumed by fuel cells, hydrogen gas turbines, or industrial processes. LOHC enables long-term and large-scale energy storage under ambient temperature and pressure conditions without

Table 1
Overview of studies on WHR strategies of LOHC chains.

References	Chain boundary (see Fig 1)	LOHC pair	Aim	Method	WHR considered	Main results
[56]	$LOHC_+$-C_{SOFC}, $LOHC_+$-C_{PEMFC}	DBT	Evaluating the integration between fuel cells and dehydrogenation of LOHC	Thermodynamic Modeling	L_--P-L_+, HC-DE	• The efficiency of dehydrogenation heat supplying methods: waste heat from high-temperature fuel cells (48.1 ± 9.6%)> combustion of hydrogen (28.7 ± 5.8%) >electric heating (13.6 ± 9.7%)
[57]	$LOHC_+$-C_{SOFC}	DBT	Assessing the performance of integrating SOFC to LOHC dehydrogenation	Experiments	L_--P-L_+, HC-DE	• The energy efficiency of the chain is 45% • LOHC vapor does not harm the operational stability of the SOFC
[58]	$LOHC_+$-C_{GT}	TOL	Assessing the performance of integrating power generation cycles to LOHC dehydrogenation	Thermodynamic Modeling	L_--P-L_+, HC-DE	• The endothermic dehydrogenation reaction is covered by the heat generated from the air-fuel combustion of H_2, and the remaining heat is supplied to the combined cycle plant for power generation • The maximum energy efficiency of the chain is 53.7%
[61]	S_{EL}-C_{PEMFC}	DBT	Assessing the performance of integrating cement plant with LOHC chain	Thermodynamic Modeling	L_+-P-L_-, L_--P-L_+, HC-DE	• The energy efficiency of the chain is increased from 15-17% using a hydrogen burner to 21.9% averaged over a month by direct coupling the LOHC dehydrogenation with the exhaust heat • By adding a thermal storage system to overcome the temperature fluctuation of the waste heat, the chain efficiency can be increased to 28.5%
[59]	$LOHC_+$-C_{INDU}	DBT, NEC, NAP, TOL, QLD, BPH, MLH, MBP	Assessing the performance of integrating LOHC dehydrogenation with the methanation process	Thermodynamic Modeling	HC-DE, HC-P-L_+	• The heat generated by the methanation process and the high-temperature exhaust gas from the gas turbine exit are utilized to supply heat for the dehydrogenation • The chain based on NEC has the highest energy efficiency (55.6%), but the DBT is considered the best selection due to its easy recovery and availability among the studied LOHCs, with an energy efficiency of 46.7%
[62]	S_{EL}-C_{PEMFC}, S_{EL}-C_{SOFC}	NEC	Assessing the feasibility of energy storage in residential and commercial buildings via LOHC	Thermodynamic modeling and techno-economic analysis	HC-DE, HC-P-L_+, HYRE	• When SOFC is the hydrogen consumer, and the SOFC heat is utilized for the dehydrogenation process, the electricity-to-electricity efficiency of the chain is 38% • When PEMFC is the hydrogen consumer, the electricity-to-electricity efficiency of the chain is 20% and 28%, respectively, when electric heating and hydrogen combustion are used to provide dehydrogenation heat
[63]	S_{EL}-C_{GT}	DBT	Evaluation of electricity storage system based on LOHC considering self-sufficient rate by renewable energy and actual energy demands	Operational modeling and economic analysis	L_+-P-L_-	• The LOHC-based electricity storage system is more cost-effective than grid purchase if >75% of the electricity demand is provided by on-site renewable energy
[53]	S_{EL}-C_{PEMFC}	DBT	Assessing the performance of the defined process chain	Net energy analysis	L_--P-L_+, HY-P-L_-	• The round-trip efficiency of the chain composed of the electrolyzers, LOHCs, and fuel cells is 28–30%
[64]	S_{EL}-C_{PEMFC}, S_{EL}-C_{GT}	DBT	Assessing the performance of a heat-control combined heating and power system fueled by natural gas with LOHC for electricity storage	Thermodynamic modeling	HC-DE, HCRE	• Technical possibilities of integrations between the LOHC system and combined heating and power system are discussed and analyzed • The integration can reduce the primary energy demand by more than 16% and significantly improve the self-sufficiency and self-consumption rate
[65]	S_{EL}-C_{SOFC}	DBT	Assessing the performance of a decentralized and self-sufficient energy system enabled by solar energy and energy storage by LOHC	Hourly dispatch modeling (Temporal optimization)	HC-DE, HCRE, HYRE	• In 2030, heat integration between a reversible solid oxide cells system and LOHC chain can enable a self-sufficient supply of electricity and heat in a single-family low-energy building at 52% higher costs compared with a system supplied by electricity from the grid • The total annualized cost of this system is 80 % lower compared to that of a system based on energy storage in a lithium-ion battery
[54]	S_{SMR}-H_{DE}	NEC	Assessing the efficiency of the defined LOHC chain	Thermodynamic modeling	HY-P-L_-, HCRE	• The energy efficiency of the LOHC chain is 69% and 89% with and without recovery of the hydrogenation heat

(*continued on next page*)

Table 1 (*continued*)

References	Chain boundary (see Fig 1)	LOHC pair	Aim	Method	WHR considered	Main results
[60]	S_{EL}-C_{SOFC}	TOL	Comparing the hydrogen supply chain enabled by ammonia and TOL	Thermodynamic modeling	L.-P-L_+	• The energy efficiency of the LOHC chain with WHR is slightly lower than the CHG chain but higher than the LH chain • The primary energy losses of the TOL chain are in the electrolysis (16%), hydrogenation (15%), and dehydrogenation (12%) • If exhaust heat can be utilized to cover the dehydrogenation heat, the total efficiency can be increased by nearly 7.5%
[66]	S_{INDU}-H_{DE}	DBT	Assessing the performance of the LOHC chain for road transport of hydrogen	Techno-economic analysis	HCRE, HYRE	• Higher hydrogen demand and especially longer transport distances favor the LOHC chain over the CHG chain • Recovery of waste heat at the hydrogen-consuming side to cover the dehydrogenation heat is a more favorable way compared with hydrogen combustion and electric heating
[7]	S_{EL}-C_{PEMFC}	DBT, NEC, NAP, TOL, FA, MET, AB	Assessing the performance of the defined LOHC chain for international hydrogen transport	Techno-economic analysis	HCRE, HYRE	• The energy efficiency of the LOHC chain mainly depends on the source of the dehydrogenation heat • For a storage time of 60 days, the LOHC chain shows economic advantages compared to the CHG chain
[55]	S_{EL}-H_{DE}	DBT, NEC, TOL, MET	Comparing the performance of the LOHC chain with alternatives for international renewable energy transport	Techno-economic analysis	HCRE	• DBT and methanol chains show the efficiency and economic advantages if the dehydrogenation heat is covered by waste heat • Long-distance transport favors LOHC, while short-distance transport via pipelines can be used for lower costs

Notes: DBT: Dibenzyltoluene(H0-DBT)/ Perhydro-dibenzyltoluene(H18-DBT).
NEC: *N*-ethylcarbazole (H0-NEC)/ Perhydro-*N*-ethylcarbazole(H12-NEC).
TOL: Toluene (H0-TOL) / Methylcyclohexane (H6-TOL)].
NAP: Naphthalene (H0-NAP)/ Decalin (*H*10-NAP).
MET: Carbon oxide (H0-MET)/ Methenol (H4-MET).
FA: Carbon oxide (H0-FA)/ Fomic acid (H2-FA).
AB: 1,2-dihydro-1,2-azaborine (H0-AB)/ a,2-BN-cyclohexan (H6-AB).
QLD: Quinaldine (H0-QLD)/ Decahydro-2-Methylquinoline (*H*10-QLD).
BPH: Biphenyl (H0-BPH)/ Bicyclohexyl (H12-BPH).
MLH: BenzyToluene (H0-MLH)/ PerhydrobenzylTolouene (H12-MLH).
MBP: 2-(*N*-Methylbenzyl)pyridine (H0-MBP)/ Perhydro product of 2-(*N*-Methylbenzyl)pyridine (H12-MB.

boil-off or other losses [7] and can be handled by today's infrastructure for liquid fuels consisting of pipelines, oil tankers, and petrol stations [29].

Previous LOHC studies mainly focused on the chemical, physical, and material aspects of LOHC hydrogenation and dehydrogenation [30–36], the estimation of thermochemical and thermophysical properties [37–47], or the development of new LOHC pairs [45–51]. However, the thermal issue also plays a vital role in the LOHC system compared with traditional methods such as CHG and LH. First, LOHC chains generate heat in the hydrogenation process and require heat for the dehydrogenation reaction. The material pair, dibenzyltoluene (H0-DBT)/Perhydro-dibenzyltoluene (H18-DBT), for example, generates 64.5 kJ of heat per mol of hydrogen, which equals 22.6 % of the higher heating value (HHV) of the stored hydrogen, in the hydrogenation reaction, and requires the same amount of heat for the dehydrogenation reaction [52]. Secondly, many hydrogen consumers, including solid oxide fuel cells (SOFC), proton exchange membrane fuel cells (PEMFC), gas turbines, and industrial processes in potential LOHC chains, generate heat. Thirdly, the loaded LOHC and the unloaded LOHC, typically stored at ambient conditions, must be preheated before the hydrogenation and dehydrogenation reactions. Finally, the loaded LOHC exiting the hydrogenation reactor and the unloaded LOHC exiting the dehydrogenation reactor have a high temperature, which can serve as a heat source. With these different heat sources and heat demands in the LOHC chains, thermal energy management and smart waste heat strategies can improve the efficiencies of LOHC chains. The following waste heat recovery (WHR) strategies have been proposed:

L_+-P-L.: Using the loaded LOHC exiting the hydrogenation reactor to preheat the entering unloaded LOHC.
L.-P-L_+: Using the unloaded LOHC exiting the dehydrogenation reactor to preheat the entering loaded LOHC.
HY-P-L.: Recovery of the hydrogenation heat to preheat the unloaded LOHC entering the hydrogenation reactor.
HC-DE: Recovery of the heat generated by the hydrogen consumer to provide the dehydrogenation heat.
HC-P-L_+: Recovery of heat generated by the hydrogen consumer to preheat the loaded LOHC entering the dehydrogenation unit.
HCRE: Recovery of the heat generated by the hydrogen consumer for heating purposes outside the LOHC chain.
HYRE: Recovery of the hydrogenation heat for heating purposes outside the LOHC chain.

Although several studies have investigated the waste heat recovery strategies in LOHC chains, the overview of these studies in Table 1 reveals that the following knowledge gaps still exist: 1) WHR potential throughout the LOHC chain from hydrogen sources to hydrogen consumers is not known. The studies assessing the whole chain efficiency never assumed WHR strategies in each chain step [7,53–55], while the studies assessing the heat integration potential for a few steps did not

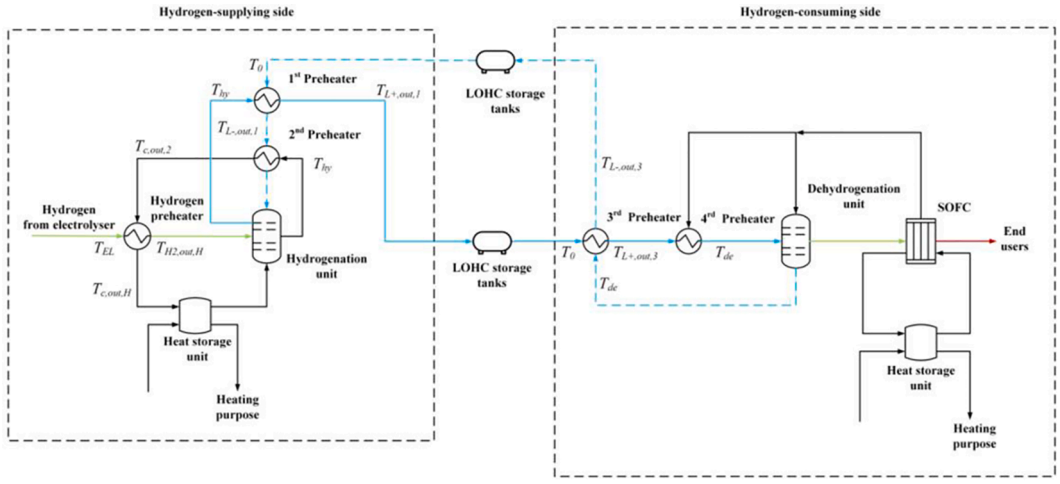

a) S_{EL}-C_{SOFC} chain

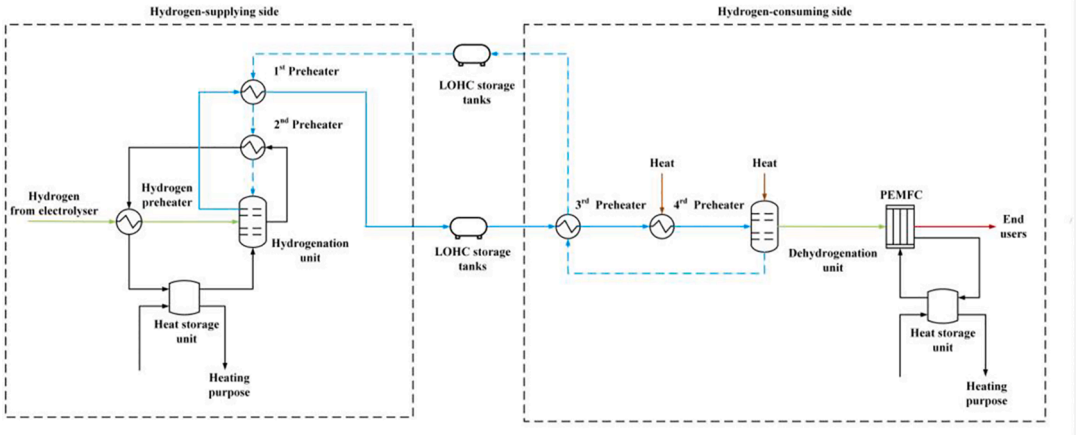

b) S_{EL}-C_{PEMFC} chain

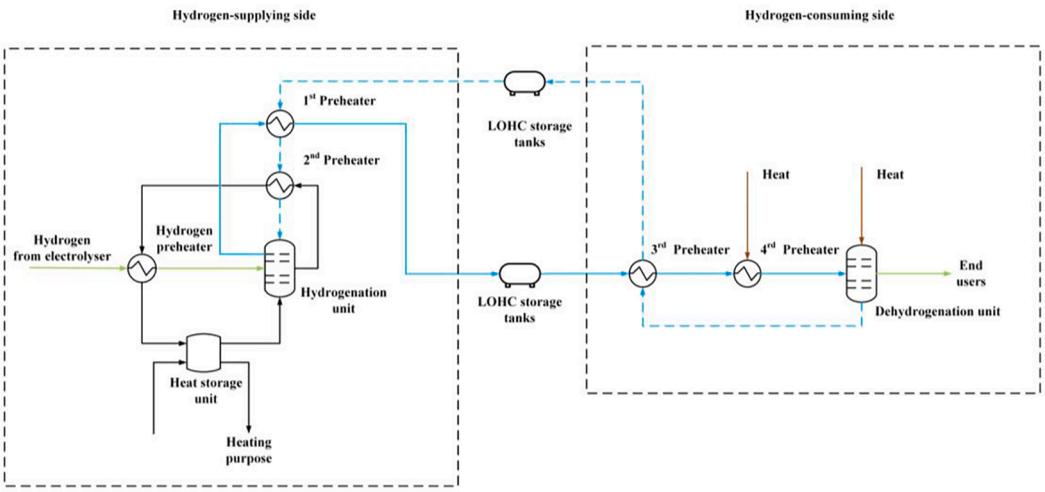

c) S_{EL}-C_{INDU} chain

Fig. 2. LOHC chains with comprehensive WHR strategies.

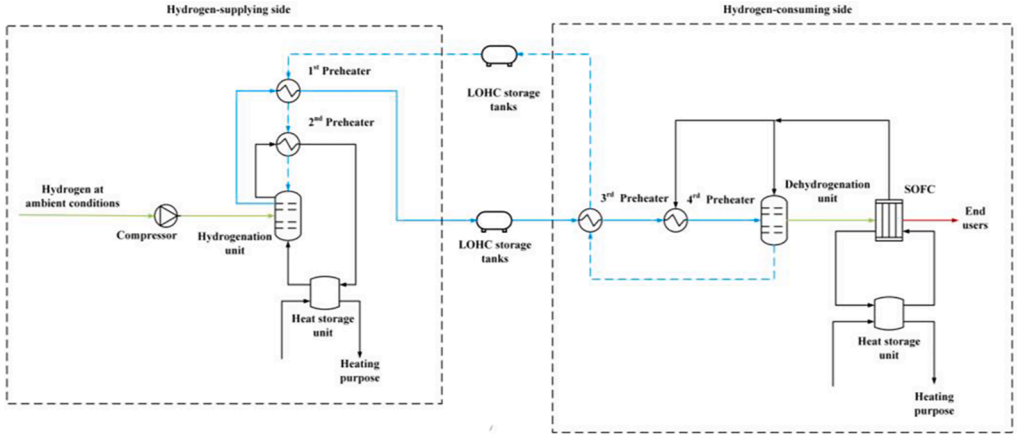

d) S_{INDU}-C_{SOFC} chain

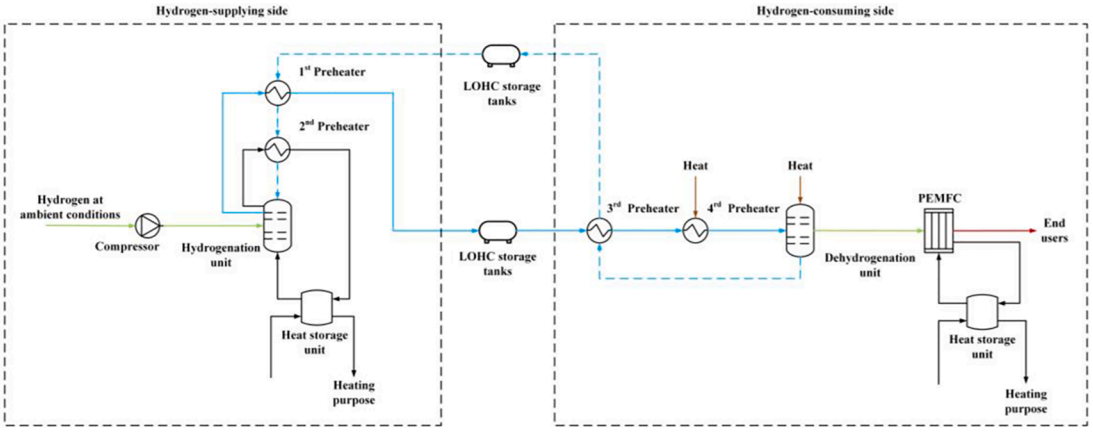

e) S_{INDU}-C_{PEMFC} chain

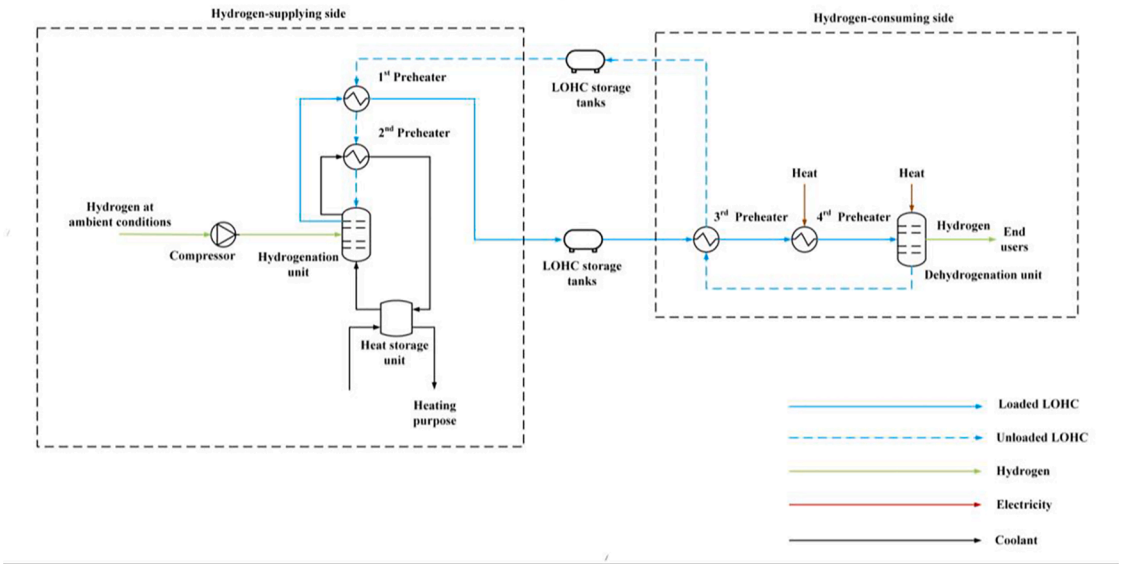

f) S_{INDU}-C_{INDU} chain

Fig. 2. (*continued*).

Table 2
Input parameters for compressor.

Parameter	Description	Value
Z	Compressibility factor	1
R	Universal gas constant	8.3145 J/mol/K
T_{suc}	Suction temperature	298.15 K
$\dot{m}_{H2.in}$	The mass flow rate of input hydrogen	0.8 kg/s
M_{H2}	The molar mass of hydrogen	2 g/mol
N	Number of compressor stages	Chain dependent with a maximum one-stage compression ratio of 2.5
k	Specific heat ratio of hydrogen	1.41
p_{hy}	Hydrogenation pressure	LOHC dependent
p_{suc}	Suction pressure	0.1 MPa
η_{me}	Mechanical efficiency	99.99 %
η_{is}	Isentropic efficiency	70 %

provide insight into the whole chain [56–59]. 2) It is unknown what the most favorable LOHC pair for implementing WHR strategies is. Although previous literature has compared different LOHCs, implementing WHR strategies can change their ranking. The reaction heat, heat capacity, and other properties of LOHC material can influence the WHR potential of the chains. 3) It is unclear which hydrogen storage method (LOHC or traditional CHG and LH) is more efficient with WHR strategies for various hydrogen sources and consumers. Previous literature focused on a defined chain but did not consider different combinations of hydrogen sources and hydrogen consumers, e.g., S_{INDU}-C_{INDU}, S_{INDU}-C_{SOFC}. 4) The information about the exergy efficiencies of LOHC chains is much limited. Several energy forms exist, i.e., heat, hydrogen, and electricity, exist in LOHC chains, which makes the exergy method that considers both energy quantity and quality a suitable tool for assessing LOHC chains. However, only one study calculated the exergy efficiency of a specific TOL-based S_{EL}-C_{SOFC} chain [60].

Therefore, the main research questions of the present study are:

(1) To what extent comprehensive WHR strategies can improve LOHC chains' efficiency?
(2) Which LOHC material enables the highest chain efficiency (energy and exergy) when implementing comprehensive WHR strategies?
(3) Which chain is more efficient with comprehensive WHR strategies among the LOHC-based and traditional hydrogen storage chains?

The main novelties and contributions are: The energy and exergy efficiencies of 24 LOHC chains, which are differentiated by two hydrogen sources, three hydrogen consumers, and four LOHC pairs, are calculated based on thermodynamic modeling. Comprehensive WHR strategies throughout the LOHC chains are designed, and the LOHC chains with and without WHR strategies are compared. Four LOHC pairs are compared when all WHR strategies are considered based on extensive data collection of the thermodynamic properties of the LOHC pairs, and the most favorable LOHC pair is determined. By comparing the LOHC chains with traditional hydrogen storage chains, the most efficient hydrogen storage method for various hydrogen chains differentiated by hydrogen sources and hydrogen consumers is determined.

2. Methods

Section 2.1 describes the 24 LOHC chains regarding hydrogen sources, hydrogen consumers, LOHC pairs, and the possible WHR strategies designed for each chain. The LOHC chains without WHR strategies and traditional chains for comparison are also defined. Section 2.2 presents the thermodynamic modeling of these chains, and the equations are solved in the EES (Engineering Equation Solver) software. Section 2.3 introduces the exergy method, and Section 2.4 defines the assessment criteria.

2.1. Chains description

2.1.1. Hydrogen sources and consumers

The temperature and pressure levels of hydrogen vary with the sources of hydrogen. This study considers two kinds of initial hydrogen sources, i.e., green hydrogen from electrolyzers and hydrogen from the industry as a by-product [65]. The latter hydrogen source needs to be compressed before the hydrogenation unit. The typical way of producing hydrogen through SMR is not considered due to its high carbon emission intensity. Three kinds of hydrogen consumers, i.e., SOFC, PEMFC, and hydrogen-fed industrial process, are considered. SOFC is considered because of its high operating temperature resulting in higher WHR potential, while PEMFC is considered due to its high technology readiness level. Combining the two hydrogen sources with three hydrogen consumers results in the LOHC chains shown in Fig. 2.

2.1.2. LOHC pairs

Many material pairs have been proposed as LOHC, but some of them are not practically feasible due to bad performance on toxicity, availability, selectivity, stability, reaction speed, and storage capacity [52]. Due to sufficient data on the thermophysical and thermochemical properties, the following four LOHC pairs are compared: DBT, NEC, TOL, and NAP.

2.1.3. WHR strategies

L + -P-L-, L–P-L+, HY-P-L-, and HCRE are applied in all the LOHC chains. In chains with S_{EL}, the hydrogenation heat is recovered to preheat the colder hydrogen from the electrolyzer. Hydrogen does not need to be preheated in chains with S_{INDU}, because it is already heated up during the compression process. In chains with C_{SOFC}, heat generated by SOFC is recovered to preheat the loaded LOHC further before the dehydrogenation unit and to satisfy the heat demand by the endothermic dehydrogenation process. The remaining heat generated by SOFC is used for external heating purposes. In chains with C_{PEMFC} or C_{INDU}, the heat demand for the dehydrogenation and the preheating of the loaded LOHC is satisfied by an electric heater. The heat generated by PEMFC is consumed for external heating purposes.

2.1.4. LOHC chains without WHR

The LOHC chains without WHR strategies are introduced to compare the difference between the efficiency of LOHC chains with and without WHR strategies. External electric heaters satisfy all the heat demands without recovery of the heat sources within these chains.

2.1.5. Traditional chains

Hydrogen can also be stored in CHG and LH, which are traditional and widely-used technologies. This study considers 6 CHG chains and 6 LH chains with the two hydrogen sources and three end-users mentioned in Section 2.1.1. Hydrogen losses do not exist in the CHG process, and liquified hydrogen boil-off is ignored.

Eq. (1) calculates the hydrogen compression work in the CHG process. The initial pressure of hydrogen is the hydrogenation pressure in CHG chains with S_{EL} and is the ambient pressure in CHG chains with S_{INDU}. In the LH chains, the energy required by the liquefaction depends on the feeding condition of hydrogen. A hydrogen liquefaction plant that liquifies hydrogen with a feeding condition of 1 bar and 300 K and a production condition of 1 bar and 20 K needs 6.93 kWh of electricity per kg H_2 [67]. However, another plant with a 60 bar and 300 K hydrogen feeding condition lower the energy consumption to 5.29 kWh/kg_{H2} with a product condition of 1.5 bar and 20 K [68]. This study assumes 6.93 and 5.29 kWh/kg_{H2} electricity consumption for hydrogen liquefaction in LH chains with, respectively, S_{EL} and S_{INDU}.

Table 3
Input parameters for the hydrogenation process [52].

LOHC	$T_{hy}(K)$	p_{hy}(bar)	q_{hy}(kJ/mol H_2)	η_{hy}(%)	Molar mass (g/mol)
H0-DBT	453.15	50	65.4	100	272
H0-NEC	453.15	70	53	100	195
H0-TOL	393.15	30	68.3	100	92
H0-NAP	573.15	69	66.3	100	128

Notes:
T_{hy}: hydrogenation temperature, p_{hy}: hydrogenation pressure, η_{hy}: hydrogenation rate.

Table 4
Input parameters for the dehydrogenation process.

LOHC	$T_{de}(K)$ [52]	p_{de}(bar) [52]	q_{de}(kJ/mol H2) [52]	η_{de}(%) [7]	Molar mass (g/mol) [52]
H18-DBT	583.15	1	65.4	97	290
H12-NEC	503.15	1	53	90	207
H6-TOL	723.15	1	68.3	95	98
*H*10-NAP	593.15	1	66.3	99	138

Notes:
T_{de}: dehydrogenation temperature, p_{de}: dehydrogenation pressure, η_{de}: hydrogenation rate.

Table 5
Parameters for fuel cells.

Parameter	SOFC [60]	PEMFC [70]
T_{FC}(K)	1023.15	353.15
η_{FC}	40.8 %	40.0 %
$\eta_{FC,h}$	38.0 %	33.0 %

2.2. Thermodynamic modeling

A static model is established to calculate the energy flows and to assess the chains' energy and exergy efficiencies. The mass flow rate of the hydrogen sources is 0.80 kg/s [7].

2.2.1. Compressors

LOHC chains with S_{EL} do not require hydrogen compression between the electrolyzer and the hydrogenation unit because the operating pressure of the electrolyzer can be set at the same or a bit higher pressure of the hydrogenation unit [53]. However, the hydrogen produced at ambient pressure for chains with S_{INDU} has to be compressed to the hydrogenation pressure. A multi-stage compressor does the hydrogen compression. Equation (1) calculates the electricity consumption by the compressors with an explanation of parameters in Table 2 [69].

$$P_{comp,H2} = \dot{m}_{H2,in}\frac{ZRT_{suc}}{M_{H2}}\frac{Nk}{k-1}\left(\left(\frac{p_{hy}}{p_{suc}}\right)^{\frac{k-1}{Nk}} - 1\right)/(\eta_{me}\eta_{is}) \quad (1)$$

2.2.2. Hydrogenation unit

The mass flow rate of the unloaded LOHC entering the hydrogenation unit can be calculated by Eq. (2).

$$\dot{m}_{L-} = \frac{\dot{m}_{H2,in}}{\partial} \bullet \frac{M_{L-}}{M_{H2}} \quad (2)$$

Where ∂ is the stoichiometric ratio of H_2 to LOHC in the hydrogenation and dehydrogenation reactions, M_{L-} is the molar mass of the unloaded LOHC.

The mass flow rate of the loaded LOHC exiting hydrogenation unit is:

$$\dot{m}_{L+} = \dot{m}_{L-} + \dot{m}_{H2,in} \quad (3)$$

The heat gerated in the hydrogenation reactor is:

$$Q_{hy} = \frac{\dot{m}_{H2,in}}{M_{H2}} \bullet q_{hy} \quad (4)$$

Where q_{hy} is the reaction heat per mole H_2 of the hydrogenation reactions, the temperature of the heat equals the operating temperature of the hydrogenation unit.

Assuming unloaded LOHC as the coolant of the hydrogenation reactor, the mass flow rate of the coolant is:

$$\dot{m}_{c,hy} = \frac{Q_{hy}}{C_{p,L+,T\_hy}\Delta T} \quad (5)$$

Where $C_{p,L+,T\_hy}$ is the mass heat capacity at a constant pressure of the loaded LOHC at hydrogenation temperature, ΔT is the temperature rise of the coolant within the hydrogenation reactor, and assumed to be 10 K.

Table 3 shows the LOHC properties for modeling the hydrogenation process. As a critical parameter determining the heat demand by LOHC preheating process, access to the heat capacity at a constant pressure of loaded and unloaded LOHCs is given special attention, as shown in **Appendix A**.

2.2.3. Dehydrogenation unit

The mass flow rate of hydrogen exiting the dehydrogenation unit is:

$$\dot{m}_{H2,out} = \frac{\dot{m}_{L+}}{M_{L+}} \bullet M_{H2} \bullet \partial \bullet \eta_{de} \quad (6)$$

Where M_{L+} is the molar mass of loaded LOHC, η_{de} is the dehydrogenation rate.

The mass flow rate of unloaded LOHC exiting the dehydrogenation unit is:

$$\dot{m}_{L-,de} = \dot{m}_{L+} - \dot{m}_{H2,out} \quad (7)$$

The heat required by the dehydrogenation unit can be calculated by:

$$Q_{de} = \frac{\dot{m}_{H2,out}}{M_{H2}} \bullet q_{de} \quad (8)$$

Where q_{de} is the reaction heat per mole H_2 of the dehydrogenation reactions.

Table 4 shows the LOHC properties for modeling the dehydrogenation process.

2.2.4. Fuel cells

The electricity generated by the fuel cell systems can be calculated by Equation (9).

$$P_{FC} = \dot{m}_{H2,out} HHV_{H2}\eta_{FC} \quad (9)$$

The waste heat generated by the fuel cell system can be calculated by Equation (10).

$$Q_{FC} = \dot{m}_{H2,out} HHV_{H2}\eta_{FC,h} \quad (10)$$

Where η_{FC} is the ratio of fuel cell electricity output to the total higher heating value of the supplied hydrogen, $\eta_{FC,h}$ is the ratio of fuel cell heat output to the total higher heating value of the supplied hydrogen, HHV_{H2} is the higher heating value of hydrogen, 142351 J/g. The temperature of the heat equals the fuel cell operating temperature.

Input parameters for modeling the fuel cells are given in Table 5.

2.2.5. Heat storage unit

Heat demand at the supplying or consuming side might not be

Table 6
Energy and exergy efficiency definition of the LOHC chains with WHR.

Chain	Exergy efficiency	Energy efficiency
S_{EL}-C_{SOFC}	$\frac{Ex_{SOFC,r}+Ex_{hy,r}+P_{SOFC}}{Ex_{H2,in}}$	$\frac{Q_{SOFC,r}+Q_{hy,r}+P_{SOFC}}{En_{H2,in}}$
S_{EL}-C_{PEMFC}	$\frac{Ex_{PEMFC,h}+P_{PEMFC}+Ex_{hy,r}}{Ex_{H2,in}+Q_{de}+Q_4}$	$\frac{Q_{PEMFC}+P_{PEMFC}+Q_{hy,r}}{En_{H2,in}+Q_{de}+Q_4}$
S_{EL}-C_{INDU}	$\frac{Ex_{H2,out}+Ex_{hy,r}}{Ex_{H2,in}+Ex_{q,de}+Ex_{Q4}}$	$\frac{En_{H2,out}+Q_{hy,r}}{En_{H2,in}+Q_{de}+Q_4}$
S_{INDU}-C_{SOFC}	$\frac{Ex_{SOFC,r}+Ex_{hy,r}+P_{SOFC}}{Ex_{H2,in}+P_{comp,H2}}$	$\frac{Q_{SOFC,r}+Q_{hy,r}+P_{SOFC}}{En_{H2,in}+P_{comp,H2}}$
S_{INDU}-C_{PEMFC}	$\frac{Ex_{PEMFC,h}+P_{PEMFC}+Ex_{hy,r}}{Ex_{H2,in}+Q_{de}+Q_4+P_{comp,H2}}$	$\frac{Q_{PEMFC}+P_{PEMFC}+Q_{hy,r}}{En_{H2,in}+Q_{de}+Q_4+P_{comp,H2}}$
S_{INDU}-C_{INDU}	$\frac{Ex_{H2,out}+Ex_{hy,r}}{Ex_{H2,in}+Ex_{q,de}+Ex_{Q4}+P_{comp,H2}}$	$\frac{En_{H2,out}+Q_{hy,r}}{En_{H2,in}+Q_{de}+Q_4+P_{comp,H2}}$

Notes:

$Ex_{SOFC,r}=Q_{SOFC,r}\left(1-\frac{T_0}{T_{SOFC}}\right)$, $Ex_{hy,r}=Q_{hy,r}(1-\frac{T_0}{T_{H2,h}})$, $En_{H2,in}=m_{H2,in}HHV_{H2}$, $En_{H2,out}=m_{H2,de}HHV_{H2}$, $Ex_{q,de}=Q_{de}(1-\frac{T_0}{T_{de}})$, $Ex_{Q4}=Q_4(1-\frac{T_0}{T_{de}})$.

synchronous with the hydrogen storage or release process, so a thermal storage unit is needed. The efficiency of the heat storage unit is 95 % [60].

2.2.6. Heat exchangers

The energy conservation equation for the 1st preheater is:

$$C_{p,L-}\dot{m}_{L-}\left(T_{L-,out,1}-T_0\right)=C_{p,L+}\dot{m}_{L+}\left(T_{hy}-T_{L+,out,1}\right)\eta_h \tag{11}$$

Where $C_{p,L-}$ is the average mass heat capacity at a constant pressure of unloaded LOHC, $C_{p,L+}$ is the average mass heat capacity at a constant pressure of unloaded LOHC, $T_{L0,out,1}$ is the temperature of unloaded LOHC exiting the 1st preheater, T_0 is the ambient temperature, 298.15 K, $T_{L+,out,1}$ is the temperature of loaded LOHC exiting the 1st preheater, η_h is the efficiency of the heat exchangers.

The minimum temperature difference of heat exchange is:

$$\Delta T_{mini}=T_{L+,out,1}-T_{L-,out,1} \tag{12}$$

The heat exchanged in 1st preheater can be calculated as:

$$Q_1=C_{p,L-}\dot{m}_{L0}\left(T_{L-,out,1}-T_0\right) \tag{13}$$

The energy conservation equation for the 2nd preheater is:

$$C_{p,L-}\dot{m}_{L-}\left(T_{L-,out,2}-T_{L-,out,1}\right)=C_{p,L+,T\_hy}\dot{m}_{c,hy}\left(T_{hy}-T_{c,out,2}\right)\eta_h \tag{14}$$

Where $T_{L-,out,2}$ is the temperature of the unloaded LOHC exiting the 2nd preheater, $T_{c,out,2}$ is the temperature of coolant exiting the 2nd preheater.

The minimum temperature difference of heat exchange is:

$$\Delta T_{mini}=T_{c,out,2}-T_{L-,out,2} \tag{15}$$

The heat exchanged in 2nd preheater can be calculated as:

$$Q_2=C_{p,L-}\dot{m}_{L-}\left(T_{L-,out,2}-T_{L-,out,1}\right) \tag{16}$$

The hydrogen sources considered in this study have a lower temperature than the hydrogenation temperature of selected LOHCs. In chains with S_{EL}, hydrogen from the electrolyzer is heated to the hydrogenation temperature by the hydrogenation heat in a hydrogen preheater [71]. The energy conservation equation for the hydrogen preheater is:

$$C_{p,H2}\dot{m}_{H2,in}\left(T_{H2,out,H}-T_{EL}\right)=C_{p,L+,T\_hy}\dot{m}_{c,hy}\left(T_{c,out,2}-T_{c,out,H}\right)\eta_h \tag{17}$$

Where T_{EL} is the operating temperature of the electrolyzer, 353.15 K, $T_{H2,out,H}$ is the temperature of the H_2 exiting the hydrogen preheater, $T_{c,out,H}$ is the temperature of coolant exiting the hydrogen preheater, $C_{p,H2}$ is the mass heat capacity at a constant pressure of hydrogen exiting the water electrolyzer.

The heat exchanged in the hydrogen preheater is:

$$Q_H=C_{p,H2}\dot{m}_{H2,in}\left(T_{H2,out,H}-T_{EL}\right) \tag{18}$$

In chains with S_{INDU}, the temperature of hydrogen sources is heated during the compression process.

The part of hydrogenation heat that can be consumed externally is:

$$Q_{hy,r}=Q_{hy}-\frac{Q_2}{\eta_h}-\frac{Q_H}{\eta_h} \tag{19}$$

The temperature of the heat source is $T_{c,out,H}$ in chains with S_{EL} and $T_{c,out,2}$ in chains with S_{INDU}.

The energy conservation equation for the 3rd preheater is:

$$C_{p,L+}\dot{m}_{L+}\left(T_{L+,out,3}-T_0\right)=C_{p,L-}\dot{m}_{L-,de}\left(T_{de}-T_{L-,out,3}\right)\eta_h \tag{20}$$

The minimum temperature difference of heat exchange is:

$$\Delta T_{mini}=T_{L-,out,3}-T_{L+,out,3} \tag{21}$$

The heat exchanged in 3rd preheater can be calculated as:

$$Q_3=C_{p,L+}\dot{m}_{L+}\left(T_{L+,out,3}-T_0\right) \tag{22}$$

For chains with C_{SOFC}, the waste heat from SOFC can be utilized to cover the LOHC preheat in the 4th preheater and dehydrogenation heat.

The heat exchanged in 4th preheater can be calculated as:

$$Q_4=C_{p,L+}\dot{m}_{L+}\left(T_{de}-T_{L+,out,3}\right) \tag{23}$$

The part of SOFC waste heat that can be consumed externally is:

$$Q_{SOFC,r}=Q_{SOFC}-Q_{de}-Q_4/\eta_h \tag{24}$$

The temperature of the waste heat is T_{SOFC}.

For chains with C_{INDU}, end-users directly consume the hydrogen without converting hydrogen into electricity. Typical end-users in these chains would be industrial processes, e.g., steel making industry. Since waste heat usually exists at the end user's side, the heat demands by the 4th preheater and the dehydrogenation unit are assumed to be satisfied by on-site waste heat at T_{de}. The waste heat consumed by the 4th preheater is Q_4.

For chains with C_{PEMFC}, high-temperature waste heat is usually not available. Therefore, external electric heaters satisfy the heat demand by the 4th preheater and the dehydrogenation unit.

As input parameters, the efficiency of the heat exchangers is 85 % [72], and the minimum temperature difference is 10 K.

2.3. Exergy model

Different energy forms, including electricity, hydrogen, and heat, are involved when evaluating the efficiency of LOHC chains, which makes the exergy method, which considers energy quantity and quality, a better option than the energy method. A standard environment should be defined first, and all subsequent calculations are based on this standard environment. This study takes the state of $T_0=298.15K$, $P_0=1$ atm as the standard environment. Mass flow exergy and energy flow exergy should be considered to conduct exergy analysis on an energy system. The mass flow exergy is the sum of physical, chemical, kinetic, and potential exergy. Since changes in kinetic exergy and potential exergy can be neglected in the present chains, the mass flow exergy is calculated as the sum of physical exergy and chemical exergy [73]:

$$Ex_m=\dot{m}e \tag{25}$$

$$e=e_{ph}+e_{ch} \tag{26}$$

$$e_{ph}=\sum[(h_i-h_0)-T_0(s_i-s_0)] \tag{27}$$

Where m is the mass flow rate, e is the mass flow exergy per unit mass flow rate, e_{ph} is the physical exergy per unit mass flow rate, e_{ch} is the

Table 7
Energy and exergy efficiency definition of the LOHC chains without WHR.

Chain	Exergy efficiency	Energy efficiency
S_{EL}-C_{SOFC}	$\frac{P_{SOFC}}{Ex_{H2,in}+Q_{preh}+Q_{de}}$	$\frac{P_{SOFC}}{En_{H2,in}+Q_{preh}+Q_{de}}$
S_{EL}-C_{PEMFC}	$\frac{P_{PEMFC}}{Ex_{H2,in}+Q_{preh}+Q_{de}}$	$\frac{P_{PEMFC}}{En_{H2,in}+Q_{preh}+Q_{de}}$
S_{EL}-C_{INDU}	$\frac{Ex_{H2,out}}{Ex_{H2,in}+Q_{preh}+Q_{de}}$	$\frac{En_{H2,out}}{En_{H2,in}+Q_{preh}+Q_{de}}$
S_{INDU}-C_{SOFC}	$\frac{P_{SOFC}}{Ex_{H2,in}+P_{comp,H2}+Q_{preh}+Q_{de}}$	$\frac{P_{SOFC}}{En_{H2,in}+P_{comp,H2}+Q_{preh}+Q_{de}}$
S_{INDU}-C_{PEMFC}	$\frac{P_{PEMFC}}{Ex_{H2,in}+Q_{preh}+Q_{de}+P_{comp,H2}}$	$\frac{P_{PEMFC}}{En_{H2,in}+Q_{preh}+Q_{de}+P_{comp,H2}}$
S_{INDU}-C_{INDU}	$\frac{Ex_{H2,out}}{Ex_{H2,in}+Q_{preh}+Q_{de}+P_{comp,H2}}$	$\frac{En_{H2,out}}{En_{H2,in}+Q_{preh}+Q_{de}+P_{comp,H2}}$

Notes:
$Q_{preh} = Q_1 + Q_2 + Q_3 + Q_4$

Table 8
Energy and exergy efficiency definition of the traditional chains with WHR.

Traditional chains	Exergy efficiency	Energy efficiency
S_{EL}-C_{SOFC}	$\frac{Ex_{SOFC}+P_{SOFC}}{Ex_{H2,in}+P_{comp}}$	$\frac{Q_{SOFC}+P_{SOFC}}{En_{H2,in}+P_{comp}}$
S_{EL}-C_{PEMFC}	$\frac{Ex_{PEMFC}+P_{PEMFC}}{Ex_{H2,in}+P_{comp}}$	$\frac{Q_{PEMFC}+P_{PEMFC}}{En_{H2,in}+P_{comp}}$
S_{EL}-C_{INDU}	$\frac{Ex_{H2,out}}{Ex_{H2,in}+P_{comp}}$	$\frac{En_{H2,out}}{En_{H2,in}+P_{comp}}$
S_{INDU}-C_{SOFC}	$\frac{Ex_{SOFC}+P_{SOFC}}{Ex_{H2,in}+P_{comp}}$	$\frac{Q_{SOFC}+P_{SOFC}}{En_{H2,in}+P_{comp}}$
S_{INDU}-C_{PEMFC}	$\frac{Ex_{PEMFC}+P_{PEMFC}}{Ex_{H2,in}+P_{comp}}$	$\frac{Q_{PEMFC}+P_{PEMFC}}{En_{H2,in}+P_{comp}}$
S_{INDU}-C_{INDU}	$\frac{Ex_{H2,out}}{Ex_{H2,in}+P_{comp}}$	$\frac{En_{H2,out}}{En_{H2,in}+P_{comp}}$

chemical exergy per unit mass flow rate, h_i is the enthalpy, h_0 is the enthalpy at the standard environment, s_i is the entropy, and s_0 is the entropy at the standard environment.

The chemical exergy of hydrogen is involved in this study, $e_{ch,H2} = 118050$ J/g.

The energy flow exergy consists of the exergy of work and heat. Exergy of work equals the value of work itself, while exergy of heat could be calculated by:

$$Ex_q = (1 - \frac{T_0}{T_s})Q \quad (28)$$

where T_s is the heat source temperature in (K), Q is the heat in (W).

2.4. Assessment criterion

2.4.1. LOHC chains with WHR

With the consideration of comprehensive waste heat recovery strategies, the energy and exergy efficiencies of the LOHC chains are defined in Table 6. The on-site waste heat in chains with C_{INDU} is regarded as input of the chain because it could have been valuable elsewhere, even if it was not utilized for the LOHC chain.

2.4.2. LOHC chains without WHR

Table 7 shows the assessment criteria of the chains without WHR. The heat demands by all the heat exchangers are satisfied by the electric heating, so this part of heat should be viewed as energy input of the chain. The efficiency of the electric heater is assumed to be 100 %, so the electricity input of the electric heater equals the heat exchanged in the preheaters in the chains with WHR. The heat generated in the fuel cells and hydrogenation reactor is wasted, so it cannot be viewed as energy output.

2.4.3. Traditional chains with WHR

Table 8 shows the assessment criteria of the traditional chains, where W_{comp} is the energy consumption of hydrogen compression in CHG process chain or the energy consumption of hydrogen liquefaction in the LH process chain. WHR is also considered in the traditional chains; heat generated by C_{SOFC} or C_{PEMFC} is assumed to be recovered for external heating purposes.

3. Results

Section 3.1 analyzes the preheating strategies with a comparison with the literature and then draws the exergy flow diagram of a typical chain. Section 3.2 compares the chains with various LOHC pairs, and Section 3.3 compares the chains with various hydrogen sources and consumers. Section 3.4 analyzes the chain efficiencies with and without WHR strategies. Section 3.5 presents an uncertainty analysis of the dehydrogenation rate and temperature.

3.1. Preheating strategies

All the chains with WHR use strategies L_+-P-L_- and HY-PL$_-$ to preheat the unloaded LOHC in all chains. The hydrogenation heat also preheats the input hydrogen in chains with S_{EL}. The temperature of the unloaded LOHC and hydrogen after the preheating strategies is examined first. Table 9 lists the parameters of fluids exiting the 1st and 2nd preheater and hydrogen preheater in the S_{EL}-C_{SOFC} chain.

At the hydrogen-supplying side, the unloaded LOHC is first heated in the 1st preheater by the loaded LOHC exiting the hydrogenation unit and then is heated in the 2nd preheater by the high-temperature coolant exiting the hydrogenation unit. Taking DBT as an example, H0-DBT can only be heated to 370.8 K in the 1st preheater and is then heated to 442.3 K in the 2nd preheater. However, the temperature of the coolant as a high-temperature fluid in the 2nd preheater is only decreased from

Table 10
Heat demands by LOHC preheating in the S_{EL}-C_{SOFC} chain with WHR strategies.

LOHC	Q_1(MW)	Q_2(MW)	Q_3(MW)	Q_4(MW)	Q_{preh}[a] (MW)	$\frac{Q_{preh}}{En_{H2,in}}$[b](%)
DBT	1.5	1.5	2.9	4.3	10.2	8.9
NEC	1.8	1.9	2.5	3.4	9.6	8.4
TOL	2.0	3.8	10.3	7.7	23.8	20.9
NAP	5.4	9.7	6.0	4.8	25.8	22.7

Notes:
[a] $Q_{preh} = Q_1 + Q_2 + Q_3 + Q_4$
[b] $En_{H2,in} = m_{H2,in}HHV_{H2} = 113.9$ MW

Table 9
The temperature of fluids exiting the 1st, 2nd, and hydrogen preheater in the S_{EL}-C_{SOFC} chain with WHR strategies.

LOHC	$T_{L-,out,1}$(K)	$T_{L-,out,2}$(K)	$T_{L+,out,1}$(K)	$T_{c,out,2}$(K)	$T_{H2,out,H}$(K)	$T_{c,out,H}$(K)
DBT	370.8	442.3	380.8	452.3	441.8	451.8
NEC	368.0	441.9	378.0	451.9	441.2	451.2
TOL	327.1	381.7	337.1	391.7	381.5	391.5
NAP	391.0	559.1	401.0	569.1	558.1	568.1

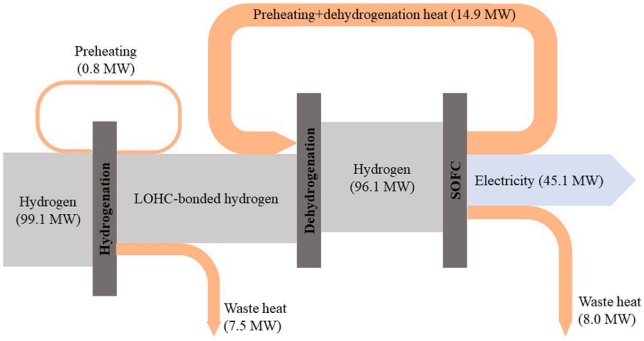

Fig. 3. Exergy flow diagram of the DBT-based S_{EL}-C_{SOFC} chain with WHR strategies.

453.2 K to 452.3 K. Then the high-temperature coolant is further cooled to 451.8 K in the hydrogen preheater. At the same time, hydrogen is preheated to 441.8 K. For various LOHCs, the temperature of unloaded LOHC and hydrogen entering the hydrogenation unit after preheating is 10.9–14.1 K and 11.4–15.1 K lower than the hydrogenation temperature, which means that the waste heat generated by the hydrogenation unit can preheat the unloaded LOHC and hydrogen to the desired temperature approaching the hydrogenation temperature.

Table 10 shows heat demands by the LOHC preheating in the S_{EL}-C_{SOFC} chain. The heat required for DBT and NEC preheating accounts for 8.9 % and 8.4 % of the input hydrogen energy, and this figure is lower than that of TOL (20.9 %) and NAP (22.7 %). The difference is that the heat capacity of TOL/NAP is higher than DBT/NEC, as seen in **Appendix A**. In addition, the dehydrogenation temperature of TOL is the highest among the LOHCs, while the hydrogenation temperature of NAP is the highest.

Fig. 3 shows the exergy flow diagram of the DBT-based chain S_{EL}-C_{PEMFC} with WHR. The recovered heat for preheating (through 1st preheater and 2nd preheater) at the hydrogen-supplying side is relatively low (0.8 MW). The amount of available waste heat that can be consumed for external heating purposes at the hydrogen-supplying side (7.5 MW) is similar to that in the hydrogen-consuming side (8.0 MW). 14.9 MW exergy is recovered for loaded LOHC preheating before dehydrogenation and endothermic dehydrogenation. The dehydrogenation process requires more exergy than the exergy generated by the hydrogenation process because the dehydrogenation temperature is higher than the hydrogenation temperature. The exergy flow diagrams of other chains and LOHC materials are not drawn, but Tables 11 and 12 provide related information.

3.2. Efficiency of one representative chain for the four selected LOHCs

Fig. 4 compares chain energy and exergy efficiencies among various LOHCs in chain S_{EL}-C_{SOFC}. The chain energy/exergy inputs and outputs, i.e., input hydrogen energy and reusable heat from hydrogenation at the hydrogen-supplying side, the electricity output by the SOFC to the end user, and reusable heat at the hydrogen-consuming side, are shown in Table 11.

The NAP chain has the highest electricity output to the end-user (46.0 MW) because of the highest dehydrogenation rate among the four LOHCs, while the NEC chain has the lowest (41.8 MW). However, the energy efficiency of the NAP chain is the lowest (57.8 %) as it requires the most heat consumption for LOHC preheating, while the energy efficiency of the NEC chain (64.7 %) is the second highest.

DBT and NEC are well-studied LOHCs that are most used in

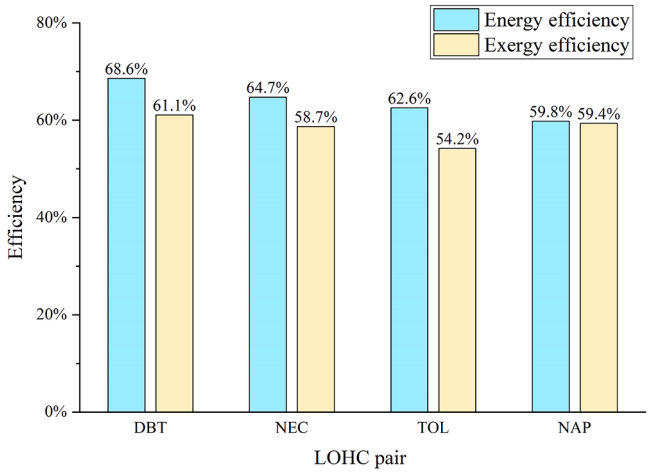

Fig. 4. Energy and exergy efficiencies of S_{EL}-C_{SOFC} chains including all WHR strategies for selected LOHCs.

Table 11
Energy and exergy input and output of S_{EL}-C_{SOFC} chains for selected LOHCs including all WHR strategies (in MW).

LOHC	Hydrogen input		Heat output at supplying side		Heat output at consuming side		Electricity output to end-user
	Energy	*Exergy*	*Energy*	*Exergy*	*Energy*	*Exergy*	*Energy/Exergy*
DBT	113.9	99.1	22.0	7.5	11.0	8.0	45.1
NEC	113.9	99.5	16.8	5.7	15.1	10.9	41.8
TOL	113.9	98.5	21.3	5.1	5.8	4.2	44.1
NAP	113.9	99.5	11.7	5.6	10.4	7.5	46.0

Table 12
Energy and exergy input and output of the DBT chains including all WHR strategies (in MW).

Chain	Hydrogen input		Hydrogen compression	Heat output at supplying side		Heat output at consuming side		External heat input	Output to end-users	
	Energy	Exergy	Energy/Exergy	Energy	Exergy	Energy	Exergy	Energy/Exergy	Energy	Exergy
S_{EL}-C_{SOFC}	113.9	99.1	0	22.0	7.5	11.0	8.0	0	45.1	45.1
S_{EL}-C_{PEMFC}	113.9	99.1	0	22.0	7.5	34.6	5.4	7.1	44.2	44.2
S_{EL}-C_{INDU}	113.9	99.1	0	22.0	7.5	0	0	7.1	110.5	91.6
S_{INDU}-C_{SOFC}	113.9	94.4	6.2	23.2	7.9	11.0	8.0	0	45.1	45.1
S_{INDU}-C_{PEMFC}	113.9	94.4	6.2	23.2	7.9	34.6	5.4	7.1	44.2	44.2
S_{INDU}-C_{INDU}	113.9	94.4	6.2	23.2	7.9	0	0	7.1	110.5	91.6

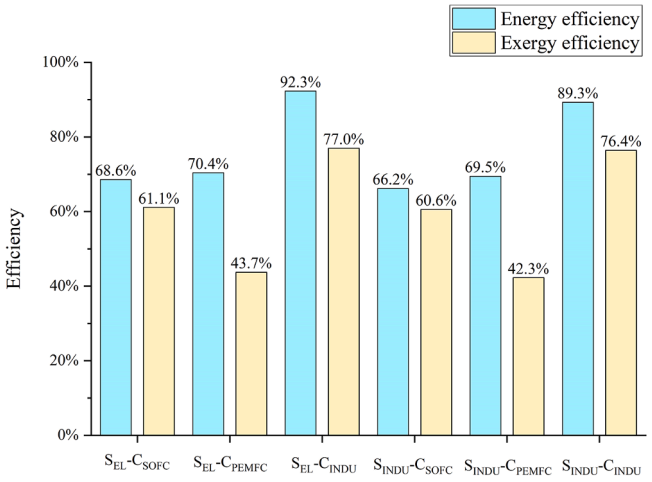

Fig. 5. Comparison of energy and exergy efficiencies among DBT chains with WHR strategies.

commercial applications. The energy efficiency of the DBT chain (68.6 %) is 4 % higher than that of the NEC chain (64.7 %), mainly because the loaded DBT has a higher dehydrogenation rate (97 %) than NEC (90 %). The difference between the exergy efficiency of DBT and NEC chains is smaller (2.4 %).

Although the energy efficiency of the NAP chain (59.8 %) is lower than that of the TOL chain (62.6 %), the exergy efficiency order is reversed mainly because the NAP's higher hydrogenation temperature leads to a higher exergy output at the hydrogen-supplying side.

3.3. Efficiency of all chains based on DBT

The energy and exergy efficiencies of the selected LOHC chains based on DBT are shown in Fig. 5, while Table 12 shows the energy/exergy inputs and outputs. The output to end-users in the last column of Table 12 is electricity output in chains with C_{PEMFC} and C_{SOFC} and is hydrogen energy output in chains with C_{INDU}.

With regard to the supply side, the energy and exergy efficiencies of S_{INDU} chains in which hydrogen is produced as a by-product are lower than those in corresponding S_{EL} chains sourced by electrolyzers, even though hydrogen needs to be preheated in the S_{EL} chains. The reason is that, unlike S_{EL} chains, S_{INDU} chains require additional energy for hydrogen compression of 6.2 MW before the hydrogenation process, which is 5.4 % of the energy content of the hydrogen input.

Regarding the demand side, the energy and exergy efficiencies of the C_{INDU} chains with the industrial consumer are higher than that of the corresponding C_{SOFC} or C_{PEMFC} chains with fuel cells. In total 91.6 MW of energy is supplied to the hydrogen-fed industrial process, which is higher than the combined electricity and heat output in the C_{PEMFC} or C_{SOFC} chains due to the energy losses in the fuel cells. In addition, the heat demand at the hydrogen-consuming side in C_{INDU} chains is satisfied by waste heat, while this heat demand needs to be met by electrical heaters in the C_{PEMFC} chains requiring electricity as input with a higher energy quality than waste heat.

The C_{PEMFC} chains and C_{SOFC} chains rank differently with regard to energy and exergy efficiencies. The energy efficiency of the C_{PEMFC} chains is slightly higher than that of C_{SOFC} chains, while the exergy efficiency of the latter is higher because the quality of the heat generated by the SOFC systems is higher than that generated by PEMFC systems.

3.4. Efficiencies with and without WHR

Fig. 6 shows the energy and exergy efficiencies of the chains with and without WHR strategies. In the S_{EL} chains, WHR strategies improve the efficiencies of the S_{EL}-C_{INDU} chain the least, with an energy efficiency increase ranging from 15.6 % to 21.7 % points and an exergy efficiency increase ranging from 8.1 % to 13.9 % points because at the hydrogen-consuming side no waste heat generated that can be recovered. The energy efficiency increase of the S_{EL}-C_{PEMFC} chain (36.5 %-40.8 % points) is the highest. The exergy efficiency increase of the S_{EL}-C_{SOFC} chain (24.5 %-29.0 % points) is the highest due to the high-temperature waste heat generated by SOFC, which can be utilized to preheat the

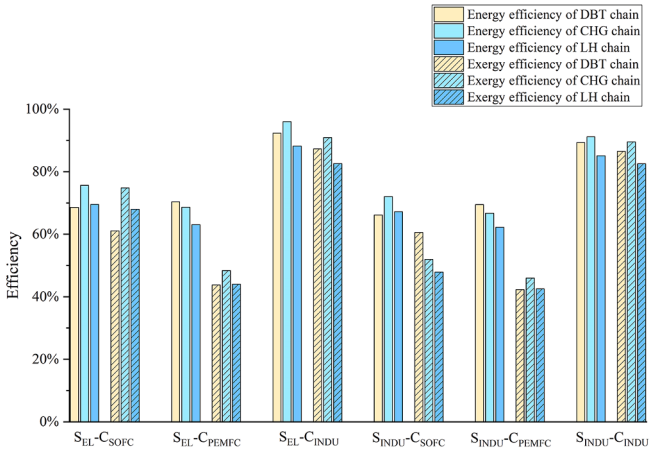

Fig. 7. Efficiencies of DBT chains and traditional chains including all WHR strategies.

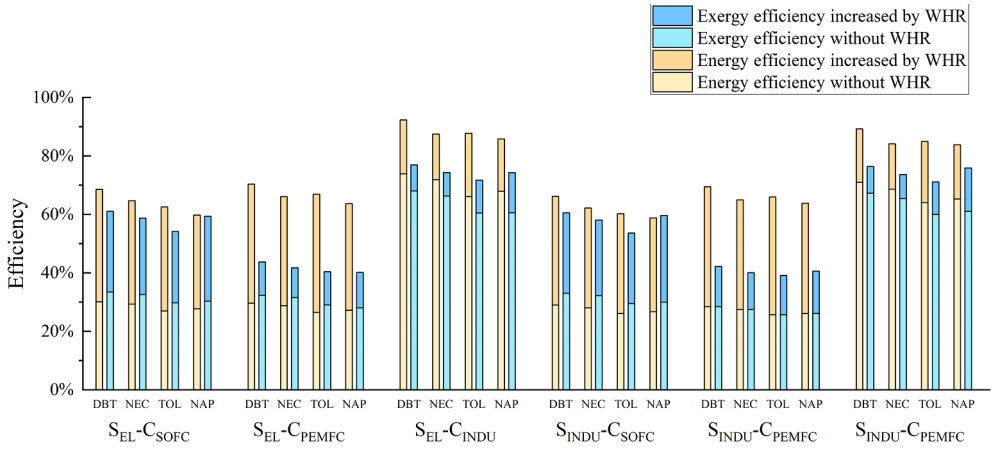

Fig. 6. Energy and exergy efficiencies of the chains with and without WHR strategies.

Table 13
Efficiency of LOHC chains under full dehydrogenation and comprehensive WHR strategies.

Chain	DBT		NEC		TOL		NAP	
	Energy	Exergy	Energy	Exergy	Energy	Exergy	Energy	Exergy
S_{EL}-C_{SOFC}	70.2 %	62.9 %	70.6 %	64.9 %	65.2 %	28.2 %	60.3 %	60.0 %
S_{EL}-C_{PEMFC}	71.7 %	44.6 %	71.0 %	45.1 %	69.0 %	41.9 %	64.1 %	40.4 %
S_{EL}-C_{INDU}	94.2 %	89.4 %	94.4 %	91.4 %	90.7 %	83.6 %	86.5 %	84.8 %
S_{INDU}-C_{SOFC}	67.8 %	62.3 %	67.8 %	64.2 %	62.8 %	56.5 %	59.3 %	60.2 %
S_{INDU}-C_{PEMFC}	70.8 %	43.1 %	69.8 %	43.3 %	68.1 %	40.6 %	64.3 %	40.9 %
S_{INDU}-C_{INDU}	91.1 %	88.6 %	90.8 %	90.4 %	87.9 %	82.8 %	84.4 %	86.8 %

Table 14
Effect of dehydrogenation temperature on the NEC-based chain efficiency with a dehydrogenation rate of 0.9 and comprehensive WHR strategies.

Efficiency		Dehydrogenation temperature (K)		
		453.15	503.15	543.15
S_{EL}-C_{SOFC}	Energy	65.5 %	64.7 %	64.1 %
	Exergy	59.4 %	58.7 %	58.2 %
S_{EL}-C_{PEMFC}	Energy	66.5 %	66.1 %	65.8 %
	Exergy	42.0 %	41.8 %	41.5 %
S_{EL}-C_{INDU}	Energy	88.0 %	87.5 %	87.1 %
	Exergy	84.8 %	83.5 %	82.5 %
S_{INDU}-C_{SOFC}	Energy	63.0 %	62.2 %	61.6 %
	Exergy	58.8 %	58.1 %	57.6 %
S_{INDU}-C_{PEMFC}	Energy	65.3 %	65.0 %	64.7 %
	Exergy	40.4 %	40.1 %	39.9 %
S_{INDU}-C_{INDU}	Energy	84.7 %	84.2 %	83.8 %
	Exergy	83.9 %	82.6 %	81.6 %

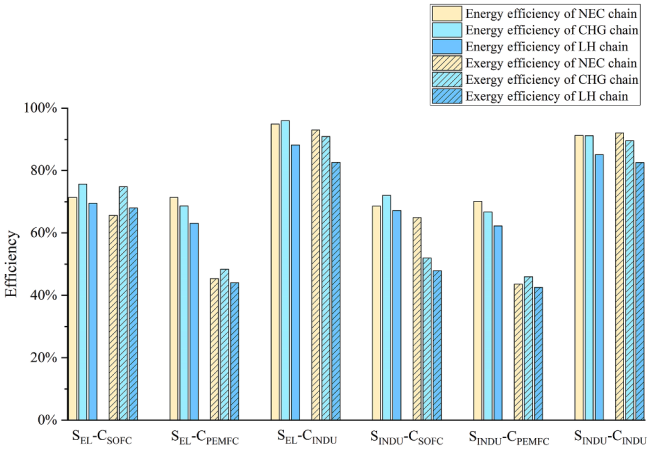

Fig. 8. Efficiencies of the most efficient NEC chains and traditional chains with all WHR strategies.

Table A1
Loaded LOHC properties for heat capacity calculation.

LOHC	$C_{p,T0}$(J/K*mol)	$C_{p,T_{de}}$(J/K*mol)	ΔH_{l-g}(J/mol)	$C_{p,L+}$(J/K*g)
H6-TOL [a]	185.3	305.7	30961@376.5 K	3.31
*H*10-NAP [a]	232.4	404.6	40658@465.8 K	3.24
H12-NEC [a]	352.1	506.7	0[a]	2.07
H18-DBT [40]	449.5	678.6	0	1.94

Notes:
a: Aspen Plus Properties

Table A2
Unloaded LOHC properties for heat capacity calculation.

LOHC	$C_{p,T0}$(J/K*mol)	$C_{p,T_{hy}}$(J/K*mol)	ΔH_{s-l}(J/mol)	ΔH_{l-g}(J/mol)	$C_{p,L0}$(J/K*g)
H0-TOL [a]	157.7	188.7	0	33240@382.7 K	5.62
H0-NAP [a]	165.7	300.3	18993@353.2 K	43237@491.6 K	5.69
H0-NEC [a]	221.6	352.1	16169@342.4 K	0	2.01
H0-DBT [40]	242.3	525.0	0	0	1.75

Notes:
a: Aspen Plus Properties

loaded LOHC and to satisfy the dehydrogenation heat at the hydrogen-consuming side. In addition, the energy quality of the heat output from SOFC is also higher than that of PEMFC. The ranking of the S_{INDU} chains with the three hydrogen consumers with regard to efficiencies improvement by WHR strategies is the same as that in the S_{EL} chains.

LOHC material is another factor that could affect the efficiency increasing rate by WHR. For example, the energy efficiency of the TOL-based S_{EL}-C_{INDU} chain is the lowest compared with the S_{EL}-C_{INDU} chain based on other LOHC material if WHR is not implemented but becomes the second largest if WHR is fully implemented. The main reason is that TOL has the highest hydrogenation heat. The exergy efficiency of the NAP-based S_{INDU}-C_{SOFC} chain is the lowest and the second largest, respectively, without and with comprehensive WHR strategies, mainly because of the high dehydrogenation temperature of *H*10-NAP which makes the energy quality of the recovered heat at hydrogen-consuming side higher.

3.5. Comparison with traditional chains

Fig. 7 compares DBT-based LOHC chain efficiency with traditional chains when WHR strategies are fully considered. For the S_{EL}-C_{SOFC} chain, the energy efficiency of the DBT chain (68.6 %) is much lower than CHG chain (75.6 %) is the highest, but only slightly lower than that of the LH chain (69.5 %). From the perspective of exergy efficiency, the differences between the DBT chain (61.1 %) and the LH chain (68.0 %) are enlarged. For the S_{INDU}-C_{SOFC} chain, the energy efficiency ranking of the studied three hydrogen storage methods is the same as that of the S_{EL}-C_{SOFC} chain, i.e., CHG-based chain > LH-based chain > DBT-based chain. However, from a perspective of exergy, the efficiency of the DBT-based chain (60.6 %) becomes the highest compared with the LH-based chain (47.9 %) and the CHG-based chain (52.0 %), which mainly results from the increased electricity input for compression by CHG chain or liquefaction by the LH chain. In addition, the high-temperature heat generated by the SOFC can be recovered to satisfy the dehydrogenation heat demand, which increases the exergy efficiency of the DBT-based

chain.

For the S_{EL}-C_{PEMFC} chain, the energy efficiency of the DBT chain (70.4 %) is the highest compared with traditional chains. However, the exergy efficiency of the CHG chain is the highest (48.4 %), while the exergy efficiency of the DBT (43.7 %) chain is slightly lower than that of the LH chain (44.0 %). For the S_{INDU}-C_{PEMFC} chain, the ranking of energy and exergy efficiencies of the studied three hydrogen storage methods is the same as that in the S_{EL}-C_{PEMFC} chain.

For the S_{EL}-C_{INDU} chain, the energy efficiency of the CHG chain (96.0 %) is the highest, while the energy efficiency of the LH chain (88.2 %) is the lowest. Also, with respect to the exergy efficiency, the CHG chain scores the best (90.9 %), and the LH chain the worst (82.6 %). The ranking of energy and exergy efficiencies of the three hydrogen storage methods in the S_{INDU}-C_{INDU} chain is the same as that in the S_{EL}-C_{INDU} chain.

3.6. Uncertainty analysis

The dehydrogenation rate of loaded LOHC can directly influence the amount of produced hydrogen with a high energy density and therefore affect the whole chain efficiency. The values of the dehydrogenation rate in Table 4 are retrieved from [7]. However, the dehydrogenation rate can vary with the dehydrogenation temperature and time, and a longer dehydrogenation duration or a higher dehydrogenation temperature usually leads to a higher dehydrogenation rate [52]. For example, a full dehydrogenation of NEC can be achieved at 543.15 K in 25 min or 453.15 K in 250 min [74,75].

Table 13 shows the energy and exergy efficiencies of the LOHC chains under full dehydrogenation and comprehensive WHR. Compared with the basic cases shown in Fig. 5, the energy and exergy efficiencies are increased under full dehydrogenation, which leads to more energy/exergy supply to the hydrogen consumer, although the heat demand by the dehydrogenation heat is increased. The NEC-based chains become more efficient than the DBT-based chains. Table 14 shows the effect of dehydrogenation temperature on the efficiency of NEC-based chains. The chains are more efficient with lower dehydrogenation temperature because both the heat demand by the loaded LOHC preheating and the exergy of the dehydrogenation heat are decreased.

Tables 13 and 14 show that the conditions for the most efficient NEC chains are full dehydrogenation and a dehydrogenation temperature of 453.15 K when WHR strategies are considered. Comparing the most efficient NEC chains with traditional chains, as shown in Fig. 8, enables the following statement:

The NEC-based chain is more efficient than the LH chain in most cases. Only in the S_{EL}-C_{SOFC} chain, NEC results in a lower exergy efficiency than LH, and only in the S_{EL}-C_{INDU} and S_{INDU}-C_{SOFC} chains, NEC results in lower energy efficiency. On the other hand, compared to the CHG storage method, NEC is less favorable and scores in three chains (S_{EL}-C_{PEMFC}, S_{INDU}-C_{PEMFC}, and S_{INDU}-C_{INDU}) better with regard to energy efficiency, and three (S_{EL}-C_{INDU}, S_{INDU}-C_{SOFC}, and S_{INDU}-C_{INDU}) with regard to exergy efficiency.

4. Discussion

This section compares the results of this study with previous literature first, then discusses this study's limitations and implications for the real world.

4.1. Literature comparison

By Aspen Plus software [62] calculated the energy efficiency of a S_{EL}-C_{SOFC} NEC chain where the heat output of SOFC is recovered to cover the dehydrogenation heat. Based on the raw data provided in [62], it can be retrieved that the hydrogen-to-electricity efficiency based on HHV of hydrogen of the S_{EL}-C_{SOFC} chain is 35.7 % under the input parameters of this study (SOFC efficiency: 40.8 %, dehydrogenation rate: 90 %), and the value in this study is 36.7 %. The result of this study fit well with [62] even though a different software/program was utilized for modeling, which can partly validate this study. The efficiencies calculated in this study vary a lot compared to that of corresponding chains in several studies [7,53,60,61], mainly because of the following variations in chain configurations: 1) whether the electrolyzer is considered part of the chain and the loss of the electrolyzer is considered or not. 2) whether the dehydrogenation heat is covered by electric heating, natural gas combustion, hydrogen combustion, or waste heat. 3) whether the losses during the transportation process are considered or not. 4) definition of assessment criteria.

The results of the preheating strategies in this study are compared with that in the literature. [53] reported that the preheating of H0-DBT to the hydrogenation temperature (423.15 K) requires 4.7 kJ heat per mole hydrogen, while it can be derived from Table 10 that the value by this study is 7.6 kJ/mol H_2. The causes for the difference include: 1) this study assumes a higher hydrogenation temperature (453.15 K) and 2) this study uses the average heat capacity of H0-DBT, which is higher than the heat capacity at 298.15 K in [53]. It was assumed that H0-DBT could be preheated to the hydrogenation temperature by hot H18-DBT without considering the actual heat exchange process in [63]. However, this study shows that part of the hydrogenation heat is needed to preheat H0-DBT further. Similarly, it was assumed that the H18-DBT could be preheated to the dehydrogenation temperature by the hot H0-DBT in [53]. The hydrogenation heat was assumed to preheat H0-DBT directly, while the heat embedded in hot H18-DBT was wasted in [54].

4.2. Caveats in this study

Assessing different LOHC chains requires a considerable amount of input data which is fully reported based on an extensive literature review. An uncertainty analysis concerning dehydrogenation rate and temperature is done. This section further elaborates on a few issues concerning this study's limitations.

- This study ignored the biol-off losses in the LH chains. It was estimated that about 1.5–3 % of hydrogen vaporizes daily because of heat input from surroundings [76]. The results in this study show the excellence of LOHC against LH with regard to efficiency in most cases, especially under full dehydrogenation. For long-term hydrogen storage, the efficiency of LH chains can be further lowered by boil-off.
- This study considers only four LOHC pairs for comparison due to the adequacy of their available thermodynamic data in the open literature, but more LOHC pairs have been proposed [45–51]. Investigating and publishing the thermodynamic properties of these materials is highly recommended, which can support the assessment of the chains based on other LOHC pairs.
- Reutilizing the compression work in a hydrogen pressure tank in the CHG-based chains is possible[77,78]. However, the utilization of the compression work is not considered because the focus of this study is the waste heat recovery of the LOHC chains, and the technology of reutilizing the compression work is not as mature as the WHR technologies.
- For the chains with hydrogen-fed industrial processes as the hydrogen consumer, heat is supplied from the industrial processes to the LOHC chains; however, the traditional chains do not require this part of heat. To make it a fair comparison among the chains, the recovered heat in the LOHC chains is considered energy input in the definition of chain efficiencies.
- The uncertainty regarding the fuel cell efficiency and heat exchanger parameters is not considered. The fuel cell efficiency causes small uncertainty in comparing the LOHC chains with traditional chains because fuel cells are part of both. The ranking between the efficiencies of chains with C_{SOFC} and C_{PEMFC} might change when the fuel

cells' efficiency is altered. The same heat exchanger parameters are used for all the chains, which causes small uncertainty to the results regarding comparison.
- This study deals only with efficiency but not the economic aspect. Techno-economic evaluation of LOHC-chains with WHR strategies is recommended for further research.
- This study assumes heat recovery within the LOHC chain for external heating purposes without considering how the heat is utilized. It is recommended to investigate the performance of integrating the thermodynamic cycles, e.g., absorption refrigeration and organic Rankine cycles, with the LOHC chains.

4.3. Implications for real world

This paper implies that WHR strategies should be considered to improve the efficiency of LOHC chains. Internally, the self-preheating of LOHC flows and heat integration between the dehydrogenation unit and end-users should always be considered. Externally, it is preferable to locate the hydrogenation in a place with sufficient heat demand.

For the selection of hydrogen storage methods for an actual project, this study implies that the DBT-based LOHC chain with WHR strategies can be the most efficient in several scenarios compared to the traditional hydrogen storage methods. Besides efficiency, the economic performance of the chains also matters a lot in the real world. The safety advantages and the possibility of reutilizing the existing infrastructure enabled by LOHC should also be considered.

5. Conclusion

24 LOHC chains, which are differentiated by hydrogen sources, end-users, and LOHC pairs, are assessed from the perspectives of energy and exergy. WHR strategies are designed for those chains to evaluate to what extent the WHR strategies can improve the chain efficiencies. The LOHC chains are also compared with traditional hydrogen storage chains based on LH and CHG technology.

WHR strategies significantly improve the LOHC chains with regard to energy and exergy efficiencies. WHR strategies can increase energy efficiency with up to 21.7 % points for the chain with hydrogen-fed industrial consumers and 40.8 % points for chains with a fuel cell as the hydrogen consumer. The exergy efficiency of the chain with hydrogen sources from the electrolyzer and PEMFC as the hydrogen consumer can improve up to 29.0 % points. However, the LOHC chains are still less efficient than the corresponding LOHC chains even if the WHR strategies are implemented except for the following cases: the DBT chain with PEMFC as the hydrogen consumer has a higher energy efficiency (70.4 % for hydrogen source from electrolyzer/69.5 % for hydrogen source as an industrial by-product) than traditional chains, including CHG (68.7 %/66.7 %) and LH chains (63.1 %/62.2 %) when WHR strategies are implemented. The exergy efficiency of the DBT chain with hydrogen sources at ambient conditions and SOFC as the hydrogen consumer is higher than the traditional hydrogen storage chains. The DBT chains with WHR strategies score higher than the LH chains in most cases, even if the boil-off loss is ignored in the LH chains.

CRediT authorship contribution statement

Longquan Li: Conceptualization, Methodology, Software, Formal analysis, Writing – original draft, Writing – review & editing. **Purushothaman Vellayani Aravind:** Supervision, Writing – original draft. **Theo Woudstra:** Supervision, Writing – original draft. **Machteld van den Broek:** Conceptualization, Supervision, Formal analysis, Writing – original draft, Writing – review & editing.

Declaration of Competing Interest

The authors declare that they have no known competing financial interests or personal relationships that could have appeared to influence the work reported in this paper.

Data availability

Data will be made available on request.

Acknowledgments

The authors would like to thank the financial support from the scholarship granted by China Scholarship Council (CSC, No.202106370021).

Appendix A. Calculation of LOHC heat capacity

A1. Heat capacity of loaded LOHC

Giving $C_{p,L+}$ as the average mass heat capacity of the loaded LOHC when the loaded LOHC is heated from T_0 to T_{de}, the heat required by the 3rd preheater and the 4th preheater is calculated as:

$$Q_3 + Q_4 = C_{p,L+} m_{L+} (T_{de} - T_0) \tag{A-1}$$

All the selected loaded LOHC materials at ambient conditions are liquid but two of them are gas at dehydrogenation temperature, i.e., TOL and NAP. Taking the enthalpy change during the phase change process into consideration, the heat required by the 3rd preheater and the 4th preheater can also be calculated as:

$$Q_3 + Q_4 = \frac{C_{p,T0} + C_{p,T_{de}}}{2} \frac{m_{L+}}{M_{L+}} (T_{de} - T_0) + \Delta H_{l-g} \frac{m_{L+}}{M_{L+}} \tag{A-2}$$

Where $C_{p,T0}$ is the molar heat capacity of loaded LOHC at ambient temperature, $C_{p,T_{de}}$ is the molar heat capacity at dehydrogenation temperature, ΔH_{l-g} is the enthalpy change of LOHC during the liquid–gas phase change process.

Combined Equation S1-1 and S1-2, we have:

$$C_{p,L+} = \left(\frac{C_{p,T0} + C_{p,T_{de}}}{2} + \frac{\Delta H_{l-g}}{T_{de} - T_0}\right) / M_{L+} \tag{A-3}$$

Properties of the loaded LOHCs as input are shown in Table A1.

A2. Heat capacity of unloaded LOHC

Giving $C_{p,L0}$ as the average mass heat capacity of the loaded LOHC when the loaded LOHC is heated from T_0 to T_{hy}, the heat required by the 1st

preheater and the 2nd preheater is calculated as:

$$Q_1 + Q_2 = C_{p,L0} m_{L0} \left(T_{hy} - T_0\right) \tag{A-4}$$

H0- NAP and H0-NEC are solid but H0-TOL and H0-DBT are liquid at ambient temperature, while H0-DBT and H0-NEC are liquid but H0-TOL and H0-NAP are gas at hydrogenation temperature. Taking the enthalpy change during the phase change process into consideration, the heat required by the 3rd preheater and the 4th preheater can also be calculated as:

$$Q_1 + Q_2 = \frac{C_{p,T0} + C_{p,T_{hy}}}{2} \frac{m_{L0}}{M_{L0}} \left(T_{hy} - T_0\right) + \left(\Delta H_{l-g} + \Delta H_{s-l}\right) \frac{m_{L0}}{M_{L0}} \tag{A-5}$$

Where $C_{p,T0}$ is the molar heat capacity of unloaded LOHC at ambient temperature, $C_{p,T_{hy}}$ is the molar heat capacity at hydrogenation temperature, ΔH_{s-l} is the enthalpy change of LOHC during the solid–liquid phase change process, ΔH_{l-g} is the enthalpy change of LOHC during the liquid–gas phase change process.

Combining equation Eq. (A1-4) with (A1-5), we have:

$$C_{p,L0} = \left(\frac{C_{p,T0} + C_{p,T_{hy}}}{2} + \frac{\Delta H_{s-l} + \Delta H_{l-g}}{T_{hy} - T_0}\right) / M_{L0} \tag{A-6}$$

Properties of the unloaded LOHCs as input are shown in Table A2.

References

[1] UNFCCC. Paris Agreement. Paris Climate Change Conference - November 20152015.
[2] UNFCCC. Glasgow Climate Pact. Glasgow Climate Change Conference - October/November 20212021.
[3] Sachs JD, Schmidt-Traub G, Williams J. Pathways to zero emissions. Nat Geosci 2016;9:799–801.
[4] IRENA. Renewable Energy Statistics 2020. 2020.
[5] IRENA. Renewable Energy Statistics 2021. 2021.
[6] IRENA. Global renwable outlook-energy transformation 2050. 2020.
[7] Niermann M, Drünert S, Kaltschmitt M, Bonhoff K. Liquid organic hydrogen carriers (LOHCs) – techno-economic analysis of LOHCs in a defined process chain. Energ Environ Sci 2019;12:290–307.
[8] Abdalla AM, Hossain S, Nisfindy OB, Azad AT, Dawood M, Azad AK. Hydrogen production, storage, transportation and key challenges with applications: a review. Energ Conver Manage 2018;165:602–27.
[9] Elbadawi AH, Ge L, Li Z, Liu S, Wang S, Zhu Z. Catalytic partial oxidation of methane to syngas: review of perovskite catalysts and membrane reactors. Catal Rev 2021;63:1–67.
[10] Garcia G, Arriola E, Chen W-H, De Luna MD. A comprehensive review of hydrogen production from methanol thermochemical conversion for sustainability. Energy 2021;217:119384.
[11] Midilli A, Kucuk H, Topal ME, Akbulut U, Dincer I. A comprehensive review on hydrogen production from coal gasification: challenges and Opportunities. Int J Hydrogen Energy 2021.
[12] Akande O, Lee B. Plasma steam methane reforming (PSMR) using a microwave torch for commercial-scale distributed hydrogen production. Int J Hydrogen Energy 2021.
[13] Ulejczyk B, Nogal Ł, Jóźwik P, Młotek M, Krawczyk K. Plasma-Catalytic Process of Hydrogen Production from Mixture of Methanol and Water. Catalysts 2021;11:864.
[14] Wu K, Dou B, Zhang H, Liu D, Chen H, Xu Y. Aqueous phase reforming of biodiesel by-product glycerol over mesoporous Ni-Cu/CeO2 for renewable hydrogen production. Fuel 2022;308:122014.
[15] Jayaraman RS, Gopinath KP, Arun J, Malolan R, Adithya S, Ajay PS, et al. Co-hydrothermal gasification of microbial sludge and algae Kappaphycus alvarezii for bio-hydrogen production: study on aqueous phase reforming. Int J Hydrogen Energy 2021;46:16555–64.
[16] Aziz M, Darmawan A, Juangsa FB. Hydrogen production from biomasses and wastes: a technological review. Int J Hydrogen Energy 2021;46:33756–81.
[17] Javed MA, Zafar AM, Hassan AA, Zaidi AA, Farooq M, El Badawy A, et al. The role of oxygen regulation and algal growth parameters in hydrogen production via biophotolysis. J Environ Chem Eng 2021:107003.
[18] Kumar R, Kumar A, Pal A. An overview of conventional and non-conventional hydrogen production methods. Mater Today: Proc 2021;46:5353–9.
[19] Wang S, Lu A, Zhong C-J. Hydrogen production from water electrolysis: role of catalysts. Nano Convergence 2021;8:1–23.
[20] Ishaq H, Dincer I. Comparative assessment of renewable energy-based hydrogen production methods. Renew Sustain Energy Rev 2021;135:110192.
[21] Capurso T, Stefanizzi M, Torresi M, Camporeale SM. Perspective of the role of hydrogen in the 21st century energy transition. Energ Conver Manage 2022;251.
[22] Kovač A, Paranos M, Marciuš D. Hydrogen in energy transition: A review. Int J Hydrogen Energy 2021.
[23] Liu W, Zuo H, Wang J, Xue Q, Ren B, Yang F. The production and application of hydrogen in steel industry. Int J Hydrogen Energy 2021;46:10548–69.
[24] Nguyen HQ, Shabani B. Proton exchange membrane fuel cells heat recovery opportunities for combined heating/cooling and power applications. Energ Conver Manage 2020;204:112328.
[25] IEA. Global Hydrogen Review 2021. 2021.
[26] Moradi R, Groth KM. Hydrogen storage and delivery: Review of the state of the art technologies and risk and reliability analysis. Int J Hydrogen Energy 2019;44:12254–69.
[27] Ullah Rather S. Preparation, characterization and hydrogen storage studies of carbon nanotubes and their composites: a review. Int J Hydrogen Energy. 2020;45:4653–72.
[28] Ahmed A, Seth S, Purewal J, Wong-Foy AG, Veenstra M, Matzger AJ, et al. Exceptional hydrogen storage achieved by screening nearly half a million metal-organic frameworks. Nat Commun 2019;10:1–9.
[29] Markiewicz M, Zhang YQ, Bösmann A, Brückner N, Thöming J, Wasserscheid P, et al. Environmental and health impact assessment of Liquid Organic Hydrogen Carrier (LOHC) systems – challenges and preliminary results. Energ Environ Sci 2015;8:1035–45.
[30] Auer F, Blaumeiser D, Bauer T, Bösmann A, Szesni N, Libuda J, et al. Boosting the activity of hydrogen release from liquid organic hydrogen carrier systems by sulfur-additives to Pt on alumina catalysts. Cat Sci Technol 2019;9:3537–47.
[31] Zhu T, Yang M, Chen X, Dong Y, Zhang Z, Cheng H. A highly active bifunctional Ru–Pd catalyst for hydrogenation and dehydrogenation of liquid organic hydrogen carriers. J Catal 2019;378:382–91.
[32] Gianotti E, Taillades-Jacquin M, Rozière J, Jones DJ. High-Purity Hydrogen Generation via Dehydrogenation of Organic Carriers: A Review on the Catalytic Process. ACS Catal 2018;8:4660–80.
[33] Sisáková K, Podrojková N, Oriňaková R, Oriňak A. Novel Catalysts for Dibenzyltoluene as a Potential Liquid Organic Hydrogen Carrier Use—A Mini-review. Energy Fuel 2021;35:7608–23.
[34] Makaryan IA, Sedov IV. Hydrogenation/Dehydrogenation catalysts for hydrogen storage systems based on liquid organic carriers (a review). Pet Chem 2021;61:977–88.
[35] Meng J, Zhou F, Ma H, Yuan X, Wang Y, Zhang J. A review of catalysts for methylcyclohexane dehydrogenation. Top Catal 2021;64:509–20.
[36] Sekine Y, Higo T. Recent trends on the dehydrogenation catalysis of Liquid Organic Hydrogen Carrier (LOHC): a review. Top Catal 2021;64:470–80.
[37] Shin BS, Yoon CW, Kwak SK, Kang JW. Thermodynamic assessment of carbazole-based organic polycyclic compounds for hydrogen storage applications via a computational approach. Int J Hydrogen Energy 2018;43:12158–67.
[38] Berger Bioucas FE, Piszko M, Kerscher M, Preuster P, Rausch MH, Koller TM, et al. Thermal Conductivity of Hydrocarbon Liquid Organic Hydrogen Carrier Systems: Measurement and Prediction. J Chem Eng Data 2020;65:5003–17.
[39] Dürr S, Zilm S, Geißelbrecht M, Müller K, Preuster P, Bösmann A, et al. Experimental determination of the hydrogenation/dehydrogenation - Equilibrium of the LOHC system H0/H18-dibenzyltoluene. Int J Hydrogen Energy 2021;46:32583–94.
[40] Müller K, Stark K, Emel'yanenko VN, Varfolomeev MA, Zaitsau DH, Shoifet E, et al. Liquid organic hydrogen carriers: thermophysical and thermochemical studies of benzyl- and dibenzyl-toluene derivatives. Ind Eng Chem Res 2015;54:7967–76.
[41] Konnova ME, Vostrikov SV, Pimerzin AA, Verevkin SP. Thermodynamic analysis of hydrogen storage: Biphenyl as affordable liquid organic hydrogen carrier (LOHC). J Chem Thermodyn 2021;159.
[42] Brooks KP, Bowden ME, Karkamkar AJ, Houghton AY, Autrey ST. Coupling of exothermic and endothermic hydrogen storage materials. J Power Sources 2016;324:170–8.
[43] Stark K, Emel'yanenko VN, Zhabina AA, Varfolomeev MA, Verevkin SP, Müller K, et al. Liquid Organic hydrogen carriers: thermophysical and thermochemical studies of carbazole partly and fully hydrogenated derivatives. Ind Eng Chem Res. 2015;54:7953–66.
[44] Aslam R, Khan MH, Ishaq M, Müller K. Thermophysical studies of dibenzyltoluene and its partially and fully hydrogenated derivatives. J Chem Eng Data 2018;63:4580–7.
[45] Verevkin SP, Siewert R, Pimerzin AA. Furfuryl alcohol as a potential liquid organic hydrogen carrier (LOHC): Thermochemical and computational study. Fuel 2020;266.

[46] Emel'yanenko VN, Varfolomeev MA, Verevkin SP, Stark K, Müller K, Müller M, et al. Hydrogen Storage: Thermochemical studies of N-Alkylcarbazoles and their derivatives as a potential liquid organic hydrogen carriers. J Phys Chem C. 2015; 119:26381–9.
[47] Verevkin SP, Siewert R, Emel'yanenko VN, Bara JE, Cao H, Pimerzin AA. Diphenyl ether derivatives as potential liquid organic hydrogen carriers: thermochemical and computational study. J Chem Eng Data. 2019;65:1108–16.
[48] Verevkin SP, Andreeva IV, Konnova ME, Portnova SV, Zherikova KV, Pimerzin AA. Paving the way to the sustainable hydrogen storage: Thermochemistry of amino-alcohols as precursors for liquid organic hydrogen carriers. J Chem Thermodyn 2021;163.
[49] Jang M, Jo YS, Lee WJ, Shin BS, Sohn H, Jeong H, et al. A High-Capacity, Reversible Liquid Organic Hydrogen Carrier: H2-Release Properties and an Application to a Fuel Cell. ACS Sustain Chem Eng 2018;7:1185–94.
[50] Li L, Yang M, Dong Y, Mei P, Cheng H. Hydrogen storage and release from a new promising Liquid Organic Hydrogen Storage Carrier (LOHC): 2-methylindole. Int J Hydrogen Energy 2016;41:16129–34.
[51] Jorschick H, Geißelbrecht M, Eßl M, Preuster P, Bösmann A, Wasserscheid P. Benzyltoluene/dibenzyltoluene-based mixtures as suitable liquid organic hydrogen carrier systems for low temperature applications. Int J Hydrogen Energy 2020;45: 14897–906.
[52] Niermann M, Beckendorff A, Kaltschmitt M, Bonhoff K. Liquid Organic Hydrogen Carrier (LOHC) – Assessment based on chemical and economic properties. Int J Hydrogen Energy 2019;44:6631–54.
[53] Lee S, Kim T, Han G, Kang S, Yoo Y-S, Jeon S-Y, et al. Comparative energetic studies on liquid organic hydrogen carrier: a net energy analysis. Renew Sustain Energy Rev 2021;150.
[54] Wang H, Zhou X, Ouyang M. Efficiency analysis of novel Liquid Organic Hydrogen Carrier technology and comparison with high pressure storage pathway. Int J Hydrogen Energy 2016;41:18062–71.
[55] Niermann M, Timmerberg S, Drünert S, Kaltschmitt M. Liquid Organic Hydrogen Carriers and alternatives for international transport of renewable hydrogen. Renew Sustain Energy Rev 2021;135.
[56] Müller K, Thiele S, Wasserscheid P. Evaluations of Concepts for the Integration of Fuel Cells in Liquid Organic Hydrogen Carrier Systems. Energy Fuel 2019;33: 10324–30.
[57] Preuster P, Fang Q, Peters R, Deja R, Nguyen VN, Blum L, et al. Solid oxide fuel cell operating on liquid organic hydrogen carrier-based hydrogen – making full use of heat integration potentials. Int J Hydrogen Energy 2018;43:1758–68.
[58] Juangsa FB, Prananto LA, Mufrodi Z, Budiman A, Oda T, Aziz M. Highly energy-efficient combination of dehydrogenation of methylcyclohexane and hydrogen-based power generation. Appl Energy 2018;226:31–8.
[59] Naseem M, Usman M, Lee S. A parametric study of dehydrogenation of various Liquid Organic Hydrogen Carrier (LOHC) materials and its application to methanation process. Int J Hydrogen Energy 2021;46:4100–15.
[60] Obara SY. Energy and exergy flows of a hydrogen supply chain with truck transportation of ammonia or methyl cyclohexane. Energy 2019;174:848–60.
[61] Krieger C, Müller K, Arlt W. Coupling of a liquid organic hydrogen carrier system with industrial heat. Chem Eng Technol 2016;39:1570–4.
[62] Teichmann D, Stark K, Müller K, Zöttl G, Wasserscheid P, Arlt W. Energy storage in residential and commercial buildings via Liquid Organic Hydrogen Carriers (LOHC). Energy Environ Sci 2012;5.
[63] Eypasch M, Schimpe M, Kanwar A, Hartmann T, Herzog S, Frank T, et al. Model-based techno-economic evaluation of an electricity storage system based on Liquid Organic Hydrogen Carriers. Appl Energy 2017;185:320–30.
[64] Haupt A, Müller K. Integration of a LOHC storage into a heat-controlled CHP system. Energy 2017;118:1123–30.
[65] Knosala K, Kotzur L, Röben FT, Stenzel P, Blum L, Robinius M, et al. Hybrid hydrogen home storage for decentralized energy autonomy. Int J Hydrogen Energy 2021;46:21748–63.
[66] Hurskainen M, Ihonen J. Techno-economic feasibility of road transport of hydrogen using liquid organic hydrogen carriers. Int J Hydrogen Energy 2020;45: 32098–112.
[67] Incer-Valverde J, Mörsdorf J, Morosuk T, Tsatsaronis G. Power-to-liquid hydrogen: exergy-based evaluation of a large-scale system. Int J Hydrogen Energy 2021.
[68] Valenti G, Macchi E. Proposal of an innovative, high-efficiency, large-scale hydrogen liquefier. Int J Hydrogen Energy 2008;33:3116–21.
[69] K.J. Damen. Reforming fossil fuel use: the merits, costs and risks of carbon dioxide capture and storage. Utrecht University, 2007.
[70] Li L, Liu Z, Deng C, Xie N, Ren J, Sun Y, et al. Thermodynamic and exergoeconomic analyses of a vehicular fuel cell power system with waste heat recovery for cabin heating and reactants preheating. Energy 2022;123465.
[71] Shi L, Qi S, Qu J, Che T, Yi C, Yang B. Integration of hydrogenation and dehydrogenation based on dibenzyltoluene as liquid organic hydrogen energy carrier. Int J Hydrogen Energy 2019;44:5345–54.
[72] Li L, Liu Z, Deng C, Ren J, Ji F, Sun Y, et al. Conventional and advanced exergy analyses of a vehicular proton exchange membrane fuel cell power system. Energy 2021;222:119939.
[73] Fallah M, Mahmoudi S, Yari M. Advanced exergy analysis for an anode gas recirculation solid oxide fuel cell. Energy 2017;141:1097–112.
[74] Brückner N, Obesser K, Bösmann A, Teichmann D, Arlt W, Dungs J, et al. Evaluation of Industrially applied heat-transfer fluids as liquid organic hydrogen carrier systems. ChemSusChem 2014;7:229–35.
[75] Yang M, Dong Y, Fei S, Ke H, Cheng H. A comparative study of catalytic dehydrogenation of perhydro-N-ethylcarbazole over noble metal catalysts. Int J Hydrogen Energy 2014;39:18976–83.
[76] Usman MR. Hydrogen storage methods: Review and current status. Renew Sustain Energy Rev 2022;167:112743.
[77] Weckerle C, Nasri M, Hegner R, Bürger I, Linder M. A metal hydride air-conditioning system for fuel cell vehicles–Functional demonstration. Appl Energy 2020;259:114187.
[78] Weckerle C, Nasri M, Hegner R, Linder M, Bürger I. A metal hydride air-conditioning system for fuel cell vehicles–Performance investigations. Appl Energy 2019;256:113957.